

1 **Title:** Hibernation reduces GABA signaling in the brainstem to enhance motor activity of  
2 breathing at cool temperatures

3 **Authors:** Sandy E. Saunders<sup>1</sup> & Joseph M. Santin<sup>1\*</sup>

4 **Affiliations:** <sup>1</sup>University of Missouri-Columbia, Division of Biological Sciences, Missouri,  
5 United States of America.

\*Email for correspondence: [santinj@missouri.edu](mailto:santinj@missouri.edu)

6

7

8

9

10

11

12

13

14

15

16

17

18

19

20

21

22

23

24 **Abstract:**

25 Background: Neural circuits produce reliable activity patterns despite disturbances in  
26 the environment. For this to occur, neurons elicit synaptic plasticity during perturbations.  
27 However, recent work suggests that plasticity not only regulates circuit activity during  
28 disturbances, but these modifications may also linger to stabilize circuits during future  
29 perturbations. The implementation of such a regulation scheme for real-life  
30 environmental challenges of animals remains unclear. Amphibians provide insight into  
31 this problem in a rather extreme way, as circuits that generate breathing are inactive for  
32 several months during underwater hibernation and use compensatory plasticity to  
33 promote ventilation upon emergence.

34 Results: Using *ex vivo* brainstem preparations and electrophysiology, we find that  
35 hibernation in American bullfrogs reduces GABA<sub>A</sub> receptor (GABA<sub>A</sub>R) inhibition in  
36 respiratory rhythm generating circuits and motor neurons, consistent with a  
37 compensatory response to chronic inactivity. Although GABA<sub>A</sub>Rs are normally critical for  
38 breathing, baseline network output at warm temperatures was not affected. However,  
39 when assessed across a range of temperatures, hibernators with reduced GABA<sub>A</sub>R  
40 signaling had greater activity at cooler temperatures, enhancing respiratory motor  
41 output under conditions that otherwise strongly depress breathing.

42 Conclusions: Hibernation reduces GABA<sub>A</sub>R signaling to promote robust respiratory  
43 output only at cooler temperatures. Although animals do not ventilate lungs during  
44 hibernation, we suggest this would be beneficial for stabilizing breathing when the  
45 animal passes through a large temperature range during emergence in the spring. More  
46 broadly, these results demonstrate that compensatory synaptic plasticity can increase  
47 the operating range of circuits in harsh environments, thereby promoting adaptive  
48 behavior in conditions that suppress activity.

49

50 **Main text:**

51 **Background**

52 Animals have the mysterious ability to produce reliable behaviors while  
53 navigating environments that should otherwise disrupt activity of the nervous system [1].  
54 This is thought to occur, in part, through a set of compensatory mechanisms that sense  
55 activity perturbations, and in turn, adjust neuronal properties to counteract the  
56 disturbance. For example, if activity falls, neurons increase synaptic excitation,  
57 decrease inhibition, and alter ion channel densities to enhance neuronal excitability [2-  
58 5]. This framework, termed “homeostatic plasticity,” has been foundational for the past  
59 30 years [6], but it has been challenging to link ethologically relevant behaviors in  
60 animals, as neurons often need to be perturbed artificially or pathologically to reveal  
61 homeostatic responses [7-12].

62 Certain organisms inhabit natural environments with potent abiotic stressors,  
63 such as pH, temperature, and hypoxia, which can cause activity challenges within the  
64 nervous system [13]. An extreme example of this problem is encountered by hibernating  
65 frogs. Like most vertebrate species, rhythmic neural circuits in the brainstem generate  
66 breathing to meet metabolic demands of the organism. However, in the cold hibernation  
67 environment frogs may spend several months underwater using only skin for gas  
68 exchange [14], while respiratory motor behavior is completely suspended [15]. To  
69 successfully emerge following months underwater, frogs employ various compensatory  
70 mechanisms to maintain these networks so that they can work effectively when needed.  
71 This includes a classic activity-dependent mechanism of compensatory plasticity called  
72 “synaptic scaling” at excitatory synapses [16, 17], and also metabolic adjustments that  
73 improve performance in hypoxia [18, 19]. As amphibians use synaptic plasticity to  
74 overcome this large environmental challenge, they provide an intriguing opportunity to  
75 understand how plasticity mechanisms are integrated within animals to promote  
76 adaptive behavior.

77 Compensatory forms of synaptic plasticity are often interpreted as a conceptually  
78 simple regulatory regime used to counteract activity disturbances (e.g., when activity  
79 goes down, excitatory synaptic strength goes up). However, experimental and modeling  
80 work indicates that when circuits are disrupted, compensatory adjustments can also  
81 “prime” circuits to perform better during future perturbations and influence the capacity  
82 for subsequent plasticity [20-22]. Thus, we hypothesized that the hibernation  
83 environment not only triggers synaptic plasticity, but also that it induces network  
84 modifications to expand the operating range in challenging environments encountered  
85 following the initial activity challenge. To test this in an ethological context, we built upon  
86 previous work demonstrating that hibernation drives apparent homeostatic plasticity at  
87 excitatory synapses [16, 17] and addressed whether inhibitory synapses contribute as  
88 well. We then asked how plasticity through inhibition influences motor function of  
89 breathing at colder temperatures, where neuronal activity is otherwise markedly  
90 suppressed. Here, we report that hibernation strongly reduced GABAergic inhibition,  
91 consistent with a classic response to chronic network inactivity [3, 23]. Despite the  
92 critical role of inhibition in this network [24], circuit function appeared surprisingly normal  
93 at warm temperatures. However, when we assessed activity across a range of  
94 temperatures, GABA<sub>A</sub>R plasticity served mainly to offset the depressive effects of acute

95 cooling, boosting the strength and frequency of motor output at lower temperatures.  
96 Given that these animals must pass through a range of temperatures as they  
97 reestablish life on land after hibernation [25, 26], network modifications that improve  
98 network activity within this range seem to play an adaptive role. Therefore, although  
99 GABAergic plasticity has no obvious impact on baseline motor function, it expands the  
100 operating range of the respiratory circuit in an otherwise suppressive environment to  
101 promote adaptive behavior.  
102

## 103 Results

104 Respiratory motor output in adult frogs is thought to arise *via* central pattern-  
105 generating mechanisms consistent with reciprocal inhibition involving GABA [24].  
106 Rhythmic activity in these premotor neurons is then carried to motor pools through  
107 interneuronal pathways that control motor outflow to respiratory muscles [27]. Activity of  
108 this network can be assessed in isolated brainstems *in vitro* which produce rhythmic  
109 motor output on a variety of cranial nerves including the trigeminal, vagal, and  
110 hypoglossal nerve root. Although the activity pattern of these nerves may differ, the  
111 output produced is largely synchronous providing a representation of the motor output  
112 that resembles lung ventilation in the whole animal [28, 29]. Here, we measured activity  
113 of the vagus nerve to monitor respiratory-related motor output from the intact brainstem  
114 preparation (cranial nerve X; CNX; schematic in Figure 1).

115  
116 To investigate plasticity in GABAergic control of the respiratory network, we first  
117 bath-applied bicuculline, a GABA<sub>A</sub> receptor antagonist, to intact brainstem preparations.  
118 Consistent with an important role for GABA<sub>A</sub>Rs in rhythmic motor activity, bicuculline  
119 caused a dose-dependent decrease in burst frequency in control brainstems at room  
120 temperature (Baseline,  $42.60 \pm 16.32$  bursts/min; 0.5  $\mu$ M Bicuculline,  $26.32 \pm 19.68$   
121 bursts/min; 1  $\mu$ M Bicuculline,  $16.86 \pm 17.03$  bursts/min; 5  $\mu$ M Bicuculline,  $5.66 \pm 3.61$   
122 bursts/min; n=5, Figure 1A,C), with most having little-to-no activity at the highest dose  
123 (10  $\mu$ M Bicuculline,  $1.74 \pm 1.10$  bursts/min; n=5, Figure 1C). Under the same  
124 experimental conditions, hibernators strongly resisted bicuculline (Baseline,  $21.12 \pm$   
125  $6.53$  bursts/min; 0.5  $\mu$ M Bicuculline,  $23.80 \pm 8.72$  bursts/min; 1  $\mu$ M Bicuculline,  $21.52 \pm$   
126  $7.71$  bursts/min; 5  $\mu$ M Bicuculline,  $14.50 \pm 5.54$  bursts/min; n=5, Figure 1B,C), with  
127 respiratory activity persisting at the highest dose (10  $\mu$ M Bicuculline,  $13.50 \pm 4.12$   
128 bursts/min; n=5, Figure 1B,C). In regard to motor amplitude, two-way ANOVA revealed a  
129 significant main effect of bicuculline on normalized motor amplitude ( $F_{(2,055, 16.44)} = 4.499$ ,  
130  $P=0.0269$ ) but not a significant effect of group or an interaction between bicuculline and  
131 group as we saw for frequency. However, this bicuculline effect is likely to be minor, as  
132 post hoc analysis showed that significantly larger bursts compared to baseline occurred  
133 at 5  $\mu$ M in controls ( $p=0.010$ ; Holm-Sidak Multiple Comparison's test), while all other  
134 comparisons to baseline were not significantly different from baseline.

135  
136 Loss of GABA<sub>A</sub>R signaling appeared to be localized to breathing circuits. In both  
137 control and hibernators, non-respiratory motor activity (long duration bursts with  
138 qualitatively different shape than respiratory bursts [30, 31]) were rare at baseline with  
139 only 1 control preparation containing these bursts. Interestingly, and despite a clear  
140 group x bicuculline interaction for respiratory burst frequency, we did not observe this  
141 same response for non-respiratory bursts (group x bicuculline interaction in two-way  
142 ANOVA;  $p=0.5373$ ). Non-respiratory bursts emerged similarly in a manner that  
143 depended on the dose of bicuculline (Figure 1A-B,D) in both controls (Baseline,  $0.04 \pm$   
144  $0.09$  bursts/min; 0.5  $\mu$ M Bicuculline,  $0.44 \pm 0.39$  bursts/min; 1  $\mu$ M Bicuculline,  $1.44 \pm$   
145  $1.05$  bursts/min; 5  $\mu$ M Bicuculline,  $3.18 \pm 0.81$  bursts/min; 10  $\mu$ M Bicuculline,  $3.08 \pm$   
146  $1.01$  bursts/min, n=5) and hibernators (Baseline,  $0.00 \pm 0.00$  bursts/min; 0.5  $\mu$ M  
147 Bicuculline,  $0.28 \pm 0.63$  bursts/min; 1  $\mu$ M Bicuculline,  $0.56 \pm 0.98$  bursts/min; 5  $\mu$ M  
148 Bicuculline,  $2.62 \pm 1.50$  bursts/min; 10  $\mu$ M Bicuculline,  $3.60 \pm 1.86$  bursts/min, n=5).

149 Given the difference in how respiratory and non-respiratory bursts alter sensitivity to  
150 bicuculline, hibernation strongly reduces the role of GABA<sub>A</sub>Rs in a way that appears  
151 specific to circuits that generate breathing but not non-respiratory behaviors.

152  
153 The previous experiment demonstrated that GABA<sub>A</sub>Rs have a strongly reduced  
154 role in the production of the respiratory rhythm after hibernation. Next, we assessed  
155 whether plasticity influenced the capacity of the respiratory network to be modulated by  
156 GABA<sub>A</sub>R activation. Therefore, we bath-applied muscimol, a GABA<sub>A</sub>R agonist, to  
157 globally activate all GABA<sub>A</sub>Rs that influence activity. In controls, the lowest dose of  
158 muscimol (500 nM) did not alter respiratory burst frequency (Baseline,  $8.27 \pm 3.7$   
159 bursts/min vs. 500 nM muscimol,  $7.20 \pm 4.0$  bursts/min; n=5). Raising the concentration  
160 to 1  $\mu$ M caused a significant decline (1  $\mu$ M muscimol,  $3.47 \pm 1.9$  bursts/min; p= 0.0282;  
161 n=5; Figure 2A,C), and exposure to 3  $\mu$ M silenced all preparations (5 out of 5). In  
162 contrast, preparations from hibernators did not significantly alter respiratory burst  
163 frequency between baseline and any dose of muscimol (Baseline,  $11.00 \pm 2.1$   
164 bursts/min; 500 nM muscimol,  $11.93 \pm 1.8$  bursts/min; 1  $\mu$ M muscimol,  $14.47 \pm 2.8$   
165 bursts/min; 3  $\mu$ M muscimol,  $6.47 \pm 7.3$  bursts/min; n=5; Figure 2B-D), with 5 out of 5  
166 preparations maintaining respiratory bursting at the highest dose. While suppression of  
167 network activity with both the antagonist and agonist may seem paradoxical, these  
168 results are consistent with the necessity of phasic inhibition for generation of respiratory  
169 activity and neuronal silencing through further activation of GABAergic inhibition,  
170 respectively. Indeed, in other circuits that use inhibition for rhythmogenesis, antagonism  
171 of GABA<sub>A</sub>Rs disrupts network dynamics required for network activity [32], while agonism  
172 of GABA<sub>A</sub>Rs also suppresses activity through membrane hyperpolarization [33]. With  
173 both agonist and antagonist experiments, these results show that hibernation leads to a  
174 large reduction in the ability of GABA<sub>A</sub>Rs to generate and modulate breathing.

175  
176 The previous experiments identify that hibernation reduces the role of GABA<sub>A</sub>Rs  
177 in generating and modulating the respiratory rhythm. At the level of the motoneuron, an  
178 activity-dependent mechanism known as “synaptic upscaling” strengthens excitatory  
179 synapses in response to hibernation [16, 17], aligning with classic homeostatic  
180 responses to chronic network inactivity [4]. Thus, we tested if hibernation also  
181 “downscales” postsynaptic GABA<sub>A</sub>Rs to reduce GABA<sub>A</sub>R inhibition. We used patch  
182 clamp electrophysiology to record miniature inhibitory postsynaptic currents (mIPSCs)  
183 carried by GABA<sub>A</sub>Rs in identified vagal motoneurons that cause breathing in  
184 amphibians. The GABA<sub>A</sub>R currents were isolated in TTX, strychnine (strych), and DNQX  
185 to block presynaptic action potentials, glycine receptors, and AMPA-glutamate  
186 receptors, respectively. GABA<sub>A</sub>R minis were recorded from a holding voltage of -60 mV.  
187 The Nernst potential for Cl<sup>-</sup> under our experimental conditions was ~5 mV; thus, inward  
188 currents in the presence of strychnine and DNQX represent minis that arise from  
189 GABA<sub>A</sub>Rs. This was confirmed in each experiment by applying bicuculline (bic) follow  
190 each recording. We did not observe changes in the mIPSC amplitude (p=0.5218;  
191 unpaired t test), charge transfer (p=0.4391; unpaired t test), rise time (p=0.1029;  
192 unpaired t test), frequency (p=0.5576; unpaired t test), as well as neuronal input  
193 resistance after hibernation (p=p=0.3647; unpaired t test) (Figure 3A-C). Therefore,



194 hibernation does not influence postsynaptic GABA<sub>A</sub>Rs and is unlikely to account for the  
195 loss of GABA<sub>A</sub>R signaling at the network level.

196

197 As the quantal GABA<sub>A</sub>R currents were unchanged on the postsynaptic  
198 motoneuron, we assessed if loss of the GABAergic tone is associated with reduced  
199 network-driven presynaptic input onto motoneurons, like that seen in sensory  
200 deprivation models of homeostatic plasticity [10, 11]. Specific respiratory synapses are  
201 not yet tractable for stimulation experiments in this system; therefore, we developed an  
202 approach to circumvent this issue. We used a novel semi-intact preparation that permits  
203 recording of individual motoneurons receiving excitation and inhibition from rhythmic  
204 premotor circuits that shape motoneuron firing of breathing (Figure 4A) [34]. As shown  
205 in Figure 4A, vagal motor neurons fire bursts of action potentials during respiratory  
206 population motor activity, reflecting activity of breathing at a single-cell resolution. Since  
207 the postsynaptic receptor density of GABA<sub>A</sub>Rs does not appear to change within these  
208 neurons after hibernation (Fig. 3), any difference in the role of GABAergic synapses for  
209 the control of motoneuron firing rate would reflect changes in network-driven  
210 presynaptic GABA release. To isolate GABA<sub>A</sub>Rs that control respiratory-related firing of  
211 motoneurons, we focally applied bicuculline to the motoneuron cell body and  
212 surrounding region *via* local pressure injection while recording its activity shaped by  
213 excitation and inhibition from rhythmic premotor inputs in the intact network. We  
214 simultaneously recorded rhythmic vagal motoneuron activity and the trigeminal nerve (a  
215 nerve that innerves the buccal floor to drive air into the lungs and activates near-  
216 synchronously with the vagal outflow) to monitor respiratory circuit output. We used the  
217 trigeminal nerve (cranial nerve V; CN V) in these experiments because physical  
218 constraints in the bath and the focal drug delivery system prevented simultaneous  
219 recording of the vagus nerve.

220

221 Motoneurons from both groups had similar average burst firing rates during  
222 breathing and resting membrane potentials in between respiratory bursts (firing rate:  
223 control, 45.26±34.8 Hz vs. hibernation, 24.19±23.0 Hz; p=0.133, unpaired t-test;  
224 membrane potential: control, -61.52 ± 4.6 mV vs. hibernation, -59.24 ± 6.5 mV,  
225 p=0.4094 unpaired t-test). In controls, local application of bicuculline led to a reversible  
226 increase in average firing frequency during the respiratory burst (Baseline, 45.26 ± 34.8  
227 Hz; Bicuculline, 89.36 ± 61.4 Hz; p<0.0001; Holm-Sidak multiple comparisons test;  
228 n=12; Figure 4B,D). This was presumably not due to changes in the chloride gradient,  
229 because two neurons in the control group that were recorded in the “loose patch”  
230 configuration, which does not disturb intracellular milieu (Fig. 4E shown in orange),  
231 more than doubled their firing rates during bicuculline exposure, aligning with data from  
232 the whole-cell mode. These results demonstrate that phasic inhibition onto motoneurons  
233 dampens firing rate during the respiratory burst. In contrast, local bicuculline had no  
234 significant effect on the firing rate of motoneurons from hibernators (Baseline, 24.19 ±  
235 23.0 Hz; Bicuculline, 38.75 ± 44.9 Hz; p=0.2629; n=9; Holm-Sidak multiple comparisons  
236 test; Figure 4C-E). Additionally, there was no change in the interburst (resting)  
237 membrane potential during focal application of bicuculline in either control (Baseline: -  
238 61.52 ± 4.6 mV; Bicuculline: -60.92 ± 4.9 mV; n=10) or hibernation groups (Baseline: -  
239 59.24 ± 6.5 mV; Bicuculline: -59.53 ± 6.5 mV; n=7), further supporting that phasic

240 respiratory-related inhibition influences motoneuron firing rate rather than a tonic  
241 GABA<sub>A</sub>R current. Taken together with the mIPSC results, network-driven GABA release  
242 appears to be reduced in a way that no longer dampens the firing rate of motoneurons  
243 during activity associated with breathing.

244  
245 These results demonstrate a critical role for GABA<sub>A</sub>Rs in generating and  
246 modulating the respiratory rhythm, as well as controlling motoneuron firing rate in  
247 control frogs. Therefore, we were surprised that baseline network frequency on average  
248 (Fig. 1C,  $p=0.2021$ ) and motor burst morphology (Figure 5) in hibernators did not  
249 change despite a rather dramatic loss of GABA<sub>A</sub>R signaling in the network. These  
250 results mirror ventilation data *in vivo*, whereby breathing frequency and breath volume  
251 were the same after hibernation [35]. Despite these similarities at warm temperatures,  
252 frogs likely need to restart breathing to some degree at temperatures around 8°C to  
253 maintain aerobic metabolism [35, 36] and then produce reliable rhythmic output at  
254 temperatures above 13°C to maintain metabolic homeostasis as they reestablish a  
255 warmer life on land [25, 26]. Yet, cold temperatures  $\leq 15^\circ\text{C}$  strongly depress the network,  
256 making it difficult to generate respiratory activity [15, 37]. Interestingly, cooling does not  
257 suppress breathing exclusively through “passive” effects on cellular properties (e.g.,  
258 slower action potentials, decreased rates of synaptic transmission), but rather, through  
259 noradrenergic signaling. Indeed, blocking  $\alpha$  adrenergic receptors blunts decreases in  
260 activity during cooling, and the actions of norepinephrine on respiratory activity in the  
261 frog brainstem are known to act through GABAergic pathways [38, 39]. This led us to  
262 test whether decreased GABA<sub>A</sub>R signaling enhances respiratory motor output at cold  
263 temperatures faced by frogs when they need to resuscitate breathing while emerging  
264 from hibernation.

265  
266 To address this, we use three groups of *ex vivo* brainstem preparations: controls,  
267 hibernators (reduced GABA signaling), and controls with GABA<sub>A</sub>Rs experimentally  
268 reduced with a subsaturating dose of bicuculline (2  $\mu\text{M}$ ). We hypothesized that control  
269 preparations with impaired GABA<sub>A</sub>R signaling would have similar responses to cooling  
270 that were like hibernators if GABA<sub>A</sub>R signaling is part of the process by which cold  
271 temperatures depress activity of the respiratory network. That is, less GABA<sub>A</sub>R signaling  
272 would cause enhanced activity at colder temperatures. First, we addressed the  
273 respiratory frequency. Cooling control brainstems from 20°C to 8°C expectedly reduced  
274 the respiratory burst frequency (Figure 6A). Interestingly, the decline in hibernators was  
275 less pronounced, with a temperature that produces 50% of baseline burst rate shifting to  
276 colder temperatures (Figure 6B). Decreasing GABA<sub>A</sub>R signaling in controls via  
277 subsaturating block of GABA<sub>A</sub>Rs also produced greater burst frequency at cold  
278 temperatures; however, this was more dramatic than hibernators, resulting in some  
279 networks with activity at 8°C (Figure 6C). Summary statistics are shown in Figure 6D.  
280 Two-way ANOVA revealed a significant temperature, group, and temperature by group  
281 interaction effect. These results were driven by several pairwise differences caused by  
282 hibernators and controls with bicuculline. Hibernators had statistically greater  
283 normalized burst frequency than controls at cooler temperatures (16°C:  $p=0.0267$ ;  
284 Holm-Sidak Multiple Comparisons test, Figure 6D blue). In addition, bicuculline  
285 application to controls had significantly greater normalized burst frequency at lower



286 temperatures (Figure 6D gray). These results are also summarized as the temperature  
287 at which burst frequency decreased by 50% ( $T_{50}$ ) (Fig 6E). Indeed, hibernators had  
288 lower  $T_{50}$  than controls, and controls with bicuculline had the lowest  $T_{50}$  values. Taken  
289 together, the network is more active at cooler temperatures when GABA<sub>A</sub>R signaling is  
290 reduced naturally by hibernation or by experimentally blocking GABA<sub>A</sub>Rs.

291  
292 In addition to respiratory frequency, we addressed the amplitude of the motor  
293 output, as this variable relates to activation of the respiratory muscles. Like frequency,  
294 cooling also depressed motor amplitude in controls, reflecting lowered motoneuron firing  
295 or recruitment during the fictive breath (Figure 6A). In hibernators and controls in the  
296 presence of bicuculline, burst amplitude appeared to be maintained across the full  
297 temperature range (Figure 6B-C). Summary statistics are shown in Figure 6F. Two-way  
298 ANOVA revealed a significant temperature, group, and temperature by group interaction  
299 effect. These results were driven by several pairwise differences in hibernators and  
300 controls with impaired GABA<sub>A</sub> signaling. Hibernators and controls with bicuculline had  
301 statistically greater burst amplitude than controls at 12°C and 10°C (12°C: hibernator vs.  
302 control:  $p=0.0276$ ; bic vs. control:  $p=0.0039$ , 10°C: hibernator vs. control:  $p=0.0254$ , bic  
303 vs. control:  $p=0.0254$ ) Holm-Sidak Multiple Comparisons test). Overall, while network  
304 output at warm temperatures were similar between controls and hibernators with  
305 reduced GABA signaling, these results demonstrate that the downregulation of GABA<sub>A</sub>R  
306 signaling by hibernation drives more robust respiratory motor activity (frequency and  
307 motor amplitude) at cooler temperatures.

308

## 309 **Discussion**

310

311 Neural circuits face constant disturbances from the environment, placing a strong  
312 pressure on plasticity mechanisms to regulate activity. Here, we corroborate previous  
313 work suggesting GABA<sub>A</sub>Rs play a role in generating the respiratory motor pattern in  
314 adult frogs and identified that they also play a distinct modulatory role to depress activity  
315 during cooling. We found that the state of hibernation triggers a downregulation of  
316 synaptic inhibition which would have been expected to cause general effects on network  
317 activity. Instead, activity of the respiratory network became more resistant to decreases  
318 in activity caused by cooling in a way that would help stabilize respiratory output as the  
319 brainstem passes through a large temperature range during emergence from the  
320 hibernation environment. Therefore, compensatory forms of synaptic plasticity can  
321 expand the operating range of circuits in challenging environments without obvious  
322 impacts on activity in unstressed conditions.

323

### 324 ***Reduced GABAergic inhibition at rhythm generating and premotor loci***

325

326 Given that the respiratory motor system undergoes a massive activity challenge  
327 (inactivity during winter [15]), mechanisms consistent with activity-dependent  
328 compensation have been predicted to play a role in maintaining network integrity to  
329 promote motor behavior in the spring [16, 17, 35]. In addition to upregulation of  
330 excitatory synaptic strength on motoneurons, here we found that hibernation strongly  
331 reduced GABA<sub>A</sub>R signaling throughout the respiratory motor network.

332 The present data lead us to suggest GABA<sub>A</sub>R plasticity at two loci within the  
333 network (Fig. 7; top panel labeled “warm”): rhythm generating circuits and motoneurons.  
334 First, expression of the respiratory rhythm in this species involves GABA<sub>A</sub>Rs [24], likely  
335 through mechanisms involving reciprocal inhibition. GABA<sub>A</sub>Rs in premotor rhythm-  
336 generating circuits must have a diminished contribution after hibernation because motor  
337 frequency in hibernators was strongly resistant to depression caused by GABA<sub>A</sub>R  
338 antagonists or agonists. Although counterintuitive, these opposing pharmacological  
339 manipulations (activating and inhibiting the receptors) both lead to suppression of the  
340 rhythm. This is likely to occur because too much inhibition depresses activity by  
341 hyperpolarizing neurons, and too little prevents phasic inhibition required for  
342 rhythmogenesis. This is reminiscent of what occurs in other species where rhythm  
343 generation depends on synaptic inhibition [32, 33]. Second, activity of the respiratory  
344 rhythm generator is transmitted through excitatory and inhibitory interneuronal pathways  
345 to recruit motoneurons that drive breathing. In contrast to inhibition’s presumed role in  
346 facilitating rhythm generation, inhibition onto motoneurons has a conventional role of  
347 constraining the firing rate during respiratory-related bursting, which is reduced after  
348 hibernation (Fig. 4). As mIPSCs carried by GABA<sub>A</sub>Rs on motoneurons were unchanged  
349 (Fig. 3), differences in presynaptic properties of inhibitory interneurons within the  
350 respiratory network likely account for weakened GABAergic control of firing (Fig. 4).  
351 Mechanistically, it is difficult at present to parse out the variables that account for the  
352 apparent loss of network-driven presynaptic GABA (*e.g.*, reduced vesicle release  
353 probability, decreased excitability of GABAergic interneurons, *etc.*), as respiratory-  
354 related synapses and GABAergic interneurons have not yet been identified in this  
355 network. Of note, rhythm and pattern generation are thought to arise, in part, from  
356 distinct populations within the respiratory central pattern generator of mammals [40]. As  
357 such, the differential effects we observed involving loss of inhibition in the respiratory  
358 circuit may stem from distinct populations within the central pattern generator itself.  
359 Overall, the specific mechanisms and network interactions await further  
360 experimentation, but the sum of our data points to the idea that rhythm-generating  
361 circuits and premotor neurons rely significantly less on GABA<sub>A</sub>Rs after hibernation.

362  
363 Given the profound loss of GABA<sub>A</sub>R signaling, which is normally required to  
364 express the respiratory rhythm, one implication of these results is that some other  
365 mechanism must take over to produce breathing after hibernation. These results align  
366 well with recent work demonstrating circuits that recently recovered from an activity  
367 challenge use a different profile of ion channels to generate similar network output  
368 under baseline conditions [20, 21]. This leads us to speculate that plasticity resulting  
369 from hibernation may switch the mechanism of rhythmogenesis from one which relies  
370 heavily on inhibition to others that use excitatory synapses or intrinsic pacemaker  
371 mechanisms [24, 41] (Fig. 7; warm panel highlight shift in rhythm generating  
372 mechanisms, circular arrows). Consistent with this idea, the amphibian respiratory  
373 network appears to use voltage-dependent pacemaker mechanisms early in  
374 development, which then is replaced by network-dependent mechanisms *via* inhibition  
375 following metamorphosis [24]. Therefore, hibernation may revert the mechanisms of  
376 rhythm generation to that seen in an earlier life stage. Indeed, other aspects of  
377 breathing such as modulation of frequency by respiratory gases also revert to a

378 juvenile-like state following hibernation [42], consistent with the idea that emerging from  
379 aquatic hibernation may share similar environmental pressures as developing air-  
380 breathing during the shift from aquatic to terrestrial habitats [43].

381

### 382 ***Reduced GABA<sub>A</sub>R signaling increases the network operating range in the cold***

383

384 The most intriguing aspect of these results was that networks operating with less  
385 GABA<sub>A</sub>R signaling after hibernation seemed to perform better at cooler temperatures  
386 (Figure 6), despite the fact that activity was largely unchanged at warm temperatures  
387 (Figure 1&5). Our data indicate that GABA<sub>A</sub>R signaling is part of the process by which  
388 cold normally depresses the frequency and amplitude of the motor output in control  
389 animals (Fig. 7; bottom panel labeled “acute cooling”). Although temperature effects on  
390 neural circuits are multifaceted, we draw this conclusion because subsaturating block of  
391 GABA<sub>A</sub>Rs in control animals opposed the typical depressive response to cooling. The  
392 mechanisms by which GABA<sub>A</sub>R signaling normally decreases activity in the cold seems  
393 to occur through two different processes. First, at the motoneuron level, cold may  
394 facilitate inhibitory GABAergic input that we showed to exist on these neurons (Figure.  
395 4) to depress the population motoneuron output (Figure 6). Thus, losing this inhibition  
396 during hibernation likely explains maintenance of the burst amplitudes across the full  
397 temperature range during acute cooling (Fig. 7, bottom right, less inhibitory input in the  
398 cold). Second, our pharmacological data suggest that GABA<sub>A</sub>R signaling plays a role in  
399 slowing breathing frequency during cooling. Therefore, the loss of this inhibition in  
400 hibernators accounts for the ability to produce stable rhythmic activity at cooler  
401 temperatures (Fig. 6E). The network-level mechanisms remain to be uncovered;  
402 however, cold temperatures activate noradrenergic neurons of the locus coeruleus [44,  
403 45], which then depress breathing frequency through  $\alpha$ -adrenoreceptors [39]. Since  
404 noradrenergic signaling depresses respiratory activity mainly through GABAergic  
405 pathways [38], modulatory mechanisms involving norepinephrine may be activated by  
406 cooling to recruit GABAergic interneurons that depress the breathing frequency at cold  
407 temperatures.

408

409 Regardless of the specific mechanism by which cold temperature and GABA<sub>A</sub>Rs  
410 interact, reduced GABA<sub>A</sub>R signaling in hibernators, therefore, serves to boost  
411 respiratory frequency and motor drive at cooler temperatures, with likely relevance for  
412 restarting breathing upon exit from hibernation as the animal passes through a range of  
413 cool temperatures (Fig. 7; bottom panel labeled “cold”). As such, we interpret plasticity  
414 of GABA<sub>A</sub>R signaling here as “homeostatic,” as it is a change in network function that  
415 opposes the activity disturbance and enhances network excitability in an environment  
416 that otherwise depresses neuronal output. The loss of GABA<sub>A</sub>R signaling after  
417 hibernation seems to explain most of the maintenance of motor amplitude across  
418 temperatures, since hibernators and controls with experimentally reduced GABA<sub>A</sub>R  
419 signaling had similar profiles across temperatures. However, despite hibernators having  
420 higher activity at lower temperatures than naïve controls, activity still dropped to a lower  
421 extent than we observed in controls with GABA<sub>A</sub>R signaling experimentally reduced  
422 (Fig. 6A-D). We speculate the quantitative differences between these two conditions  
423 might point to additional plasticity mechanisms that tamp down enhanced excitability at

424 cold temperatures to prevent ectopic breaths while submerged in cold water. While the  
425 mechanisms that serve this purpose are not fully known, we have shown that sensory  
426 input from CO<sub>2</sub>/pH chemoreceptors that normally stimulate breathing is reduced in  
427 hibernators [35, 42], suggesting that hibernation may also reduce excitability in some  
428 parts of the network to help keep breathing off until it is needed. The exact “switch” that  
429 restarts breathing also remains unclear, but nevertheless, our results suggest that the  
430 loss of GABA<sub>A</sub>R signaling prepares the network to produce strong motor bursting at cool  
431 temperatures when it does restart, which would likely contribute to restoring breathing  
432 as the animal passes through a range of colder temperature before returning to a  
433 warmer body temperature after emergence.

434

### 435 ***Conclusions: What does it mean for plasticity to be “homeostatic?”***

436

437 Since its inception [6], compensatory mechanisms within the theme of  
438 homeostatic regulation are most often portrayed as a conceptually simple (but  
439 mechanistically complex) counterbalancing of altered excitability. Our results provide  
440 evidence that mechanisms consistent with homeostatic plasticity can increase the  
441 operating range of circuits in harsh environments that otherwise disrupt activity. We  
442 acknowledge that a strict definition of “homeostatic plasticity” might not encompass the  
443 plasticity we observed. Through a homeostatic lens, one might expect network activity  
444 that drives lung ventilation to restart as compensation enhances network excitability.  
445 However, breathing does not restart during hibernation [15], which in itself seems  
446 important for animal survival as restarting breathing prematurely could be detrimental  
447 underwater. In addition, the integrated output of the entire respiratory network does not  
448 appear obviously hyperexcitable after emergence, as breathing in vivo is comparable  
449 between controls and hibernators, which could be interpreted as inconsistent with  
450 homeostatic theory [35]. While our observations deviate from traditional definitions of  
451 negative feedback homeostasis on which the field was founded [4, 6, 46], reduced  
452 GABA<sub>A</sub>R signaling indeed increases the strength and frequency of respiratory motor  
453 activity in cool conditions that must be passed through to reestablish life on land after  
454 hibernation, thereby widening the circuit’s operating range across temperatures.  
455 Intriguingly, hibernation also leads to enhanced desensitization and reduced Ca<sup>2+</sup>  
456 permeability of NMDA receptors that serves to constrain excitability of this network  
457 during severe hypoxia that occurs as the animal emerges, with no impact on baseline  
458 activity of the network [47]. Therefore, multiple forms of synaptic plasticity appear to be  
459 masked at baseline, but ultimately increase the operating range for motor activity under  
460 the variety of stressors that occur during emergence from the hibernation environment.  
461 Overall, these results support the view that circuits may implement compensatory  
462 mechanisms in ways that enhance activity under specific sets of environmental  
463 constraints. These findings may have important implications for diverse neural systems,  
464 as the nervous system of most animals operate homeostatically over a range of abiotic  
465 conditions, such as changes in local tissue temperature [48], pH [49, 50], oxygen levels  
466 [47], hormonal state, and other factors that have the potential to disrupt network activity  
467 on acute timescales. By linking plasticity to a challenging environment in vivo, our



468 results lead us to emphasize that frameworks seeking to link compensation to behavior  
469 must ultimately incorporate how plasticity is integrated over the range of environments  
470 that neural circuits may encounter. Understanding how the nervous system is tuned to  
471 survive extreme conditions in intact animals will continue to provide new insights along  
472 this path.

473

## 474 **Methods**

475 **Animals** All experiments performed were approved by the Animal Care and Use  
476 Committee (ACUC) at the University of Missouri (protocol #39264). Adult Female  
477 American Bullfrogs (~100 g weight, n= 62), *Lithobates catesbeianus*, were purchased  
478 from Rana Ranch (Twin Falls, Idaho) and were housed in 20-gallon plastic tanks  
479 containing dechlorinated water at room temperature bubbled with room air. Control frogs  
480 were acclimated for 1 week following arrival before experiments. Frogs had access to  
481 wet and dry areas. Frogs were maintained on a 12-hour light/dark cycle and fed once  
482 per week. Water was cleaned daily and changed weekly. Hibernated frogs were kept in  
483 plastic tanks under the same conditions (exception of food being withheld) as control  
484 frogs for > 1 week before temperature was gradually lowered to 4°C over 10 days in a  
485 walk-in temperature-controlled environmental chamber. Once water temperature  
486 reached 4°C, air access was blocked using a plastic screen placed in the tank. After 4  
487 weeks of submergence, experiments commenced.

488

## 489 **Drugs**

490 Strychnine hydrochloride was from Sigma-Aldrich (St Louis, MO, USA). (-)-Bicuculline  
491 methiodide, tetrodotoxin citrate, DNQX disodium salt, and Muscimol were from Hello Bio  
492 (Princeton, NJ, USA).

493

## 494 **Brainstem-spinal cord preparation**

495 Brainstem-spinal cord preparations were generated as previously described [16]. Briefly,  
496 frogs were deeply anesthetized with isoflurane until visible respirations had ceased and  
497 response to foot pinch was absent. Frogs were then decapitated with a guillotine. The  
498 head was submerged in ice-cold bullfrog artificial cerebrospinal fluid (aCSF;  
499 concentrations in [mM]: 104 NaCl, 4 KCl, 1.4 MgCl<sub>2</sub>, 7.5 glucose, 40 NaHCO<sub>3</sub>, 2.5  
500 CaCl<sub>2</sub> and 1 NaH<sub>2</sub>PO<sub>4</sub>, and bubbled with 98.5% O<sub>2</sub>, 1.5% CO<sub>2</sub>; pH = 7.85) and the  
501 forebrain was pithed. The brainstem-spinal cord was then carefully removed, keeping  
502 nerve roots intact. Following the dissection, the brainstem was transferred to a chamber  
503 superfused with oxygenated aCSF. In a subset of experiments where bicuculline was  
504 bath applied to the *in vitro* preparation (described below), brainstems were transected at  
505 the spinomedullary junction before recording to avoid the contribution of spinal motor  
506 populations to non-respiratory motor activity induced through disinhibition [51]. Cranial  
507 nerve X (vagus) activity was recorded using glass suction electrodes immediately  
508 following dissection. Recordings were AC amplified (1000x, A–M Systems Model 1700,  
509 A–M Systems, Carlsborg, WA, USA), filtered (10 Hz – 5 kHz), and digitized (Powerlab  
510 8/35 ADInstruments, Colorado Springs, CO, USA). Nerve activity was rectified and

511 integrated (time constant =100 ms) online to allow for visualization of nerve output  
512 pattern.

513  
514 Vagus nerve output was then allowed to stabilize for  $\geq 1$  hour before drug application. In  
515 a subset of experiments (n=10 bullfrogs, 5 per group), various doses of bicuculline (500  
516 nM, 1  $\mu$ M, 5  $\mu$ M, 10  $\mu$ M), a GABA<sub>A</sub> receptor antagonist, were superfused for 10  
517 minutes in order of increasing concentration and then washed out. In a different subset  
518 of experiments (n=10 bullfrogs, 5 per group), various doses (500 nM, 1  $\mu$ M, 3  $\mu$ M) of  
519 muscimol, a GABA<sub>A</sub> receptor agonist, were added to the perfusate. Each dose was  
520 superfused for 10 minutes in order of increasing concentration. Bicuculline (10  $\mu$ M)  
521 was added to the perfusate following muscimol to reverse muscimol's effects serving as  
522 a control that output depression was not due to some kind of drift over time, but rather  
523 activation of GABA<sub>A</sub> receptors.

524  
525 For temperature experiments, preparations were allowed to recover for ~1 hr at 22°C  
526 before exposure to the temperature ramp from 20° to 8°C. Preparations from controls  
527 (n=5) and hibernators (n=6) were cooled to each temperature for 10 minutes and then  
528 the temperature was lowered by 2°C. Following cooling, preparations were rewarmed  
529 on a continuous ramp that lasted approximately 5 min. Separate control preparations  
530 (n=5) were treated with 2  $\mu$ M bicuculline for 30 minutes prior to starting the cooling  
531 ramp. 2  $\mu$ M was selected as it was the highest dose where respiratory-related bursts  
532 were prominent in controls. The temperature was controlled by a Warner Instruments  
533 bipolar in-line temperature controller (model CL-100; Hamden, CT), and chamber  
534 temperature was monitored directly next to the brainstem.

### 535 536 **Dye labeling of vagal motor neurons**

537 Brainstems were isolated as described above. In a different group of experiments,  
538 following isolation, brainstems were transferred to a chamber superfused with  
539 oxygenated aCSF. The 4<sup>th</sup> branch of the vagal nerve root, which primarily innervates the  
540 glottal dilator [52] was then isolated and suctioned into a glass pipette (bilaterally).  
541 Fluorescent dextran dye dissolved in PBS (tetramethylrhodamine 3000 MW lysine  
542 fixable dye; Invitrogen – Thermo Fisher, Waltham, MA, USA) was then backfilled into  
543 both pipettes and left to diffuse into the nerve root for 2 hours. This generated robust  
544 labeling of vagal motor neurons as previously described [16].

### 545 546 **Semi-intact brainstem-spinal cord preparation**

547 Following dye labeling, in a subset of experiments (n=15 bullfrogs) the brainstem was  
548 embedded into agarose and sliced, similar to previously described [33] with some  
549 modifications. Briefly, partially cooled, but not solidified, agarose was pipetted into a thin  
550 layer onto a scored (with fine forceps) agar block. The brainstem was then dragged onto  
551 the agarose-covered agar block, laying horizontally dorsal side up. Agarose (~57° C)  
552 was pipetted onto the top of the brainstem caudal to obex. The agar block was then  
553 mounted on a vibrating microtome plate (Campden Vibrating Microtome 7000smz,  
554 Campden Instruments; Lafayette, IN, USA) and covered in ice-cold bubbled aCSF. The  
555 blade was zeroed at the top of the brainstem, then slices were taken caudal to rostral,  
556 stopping shortly rostral to obex which was approximately 1/3 of the distance from the



557 hypoglossal root to the vagal root and spanned a fraction of the vagal motor pool extent.  
558 The blade was removed after each slice and the resulting attached slice was trimmed  
559 off the brainstem with fine spring scissors. Approximately 650  $\mu\text{m}$  were removed from  
560 the dorsal surface in total, providing access to labeled motor neurons for recording. The  
561 brainstem was removed from the remaining agar and transferred to a 35 mm glass  
562 bottom sylgard-coated dish with a stainless-steel mesh insert. The brainstem was then  
563 pinned dorsal side up. The dish was placed in a QE-1 platform (Warner Instruments,  
564 Holliston, MA, USA) that was mounted on a fixed stage microscope (FN1, Nikon  
565 Instruments Inc., Melville, NY, USA). Once on the rig, the preparation was  
566 superfused with bubbled aCSF either using gravity or with a peristaltic pump (Rainin  
567 Rabbit). The trigeminal nerve (CN V) was recorded using a glass suction electrode to  
568 monitor preparation output over time. Nerve recordings were AC amplified (1000x, A–M  
569 Systems Model 1700, A–M Systems, Carlsborg, WA, USA), filtered (10 Hz – 5 kHz), and  
570 digitized (Powerlab 8/35 ADInstruments, Colorado Springs, CO, USA). The trigeminal  
571 nerve was recorded instead of the vagal nerve root because of physical constraints in  
572 the bath with the patch pipette and picospritzer pipette used in experiments described  
573 below. The trigeminal provides a sufficient surrogate for efferent respiratory motor  
574 output [29, 53], as respiratory activity of the trigeminal and vagus nerves activate near-  
575 synchronously *in vitro*. Labeled motor neurons were then located and visualized using  
576 an imaging camera (Hamamatsu ORCA Flash 4.0LT sCMOS, Hamamatsu Photonics,  
577 Hamamatsu City, Japan) coupled to Nikon imaging software (NIS elements).

578  
579 Whole-cell recordings were made from labeled vagal motor neurons with an Axopatch  
580 200B amplifier (Molecular Devices) in current-clamp mode ( $I=0$ ). Cells were selected  
581 based on firing pattern, that is only cells that fired spontaneous bursts of action  
582 potentials or increased firing frequency (respiratory modulated) during respiratory motor  
583 bursts were sampled, as these neurons likely innervate the glottal dilator of bullfrogs  
584 [54], which is critical to permit airflow into the lungs of bullfrogs during ventilation and as  
585 such remains inactive during hibernation. Accordingly, neurons with subthreshold  
586 respiratory input or neurons that were active only during the interburst interval were  
587 excluded from testing. Glass pipettes ( $\sim 4\text{--}7\text{ M}\Omega$ ) were filled with a solution containing (in  
588 mmol): 110 potassium gluconate, 2  $\text{MgCl}_2$ , 10 Hepes, 1  $\text{Na}_2\text{-ATP}$ , 0.1  $\text{Na}_2\text{-GTP}$  and 2.5  
589 EGTA, pH  $\sim 7.2$  with KOH. Data were acquired in pClamp 11 software using an  
590 Axopatch 200B amplifier and Axon Digidata 1550B digitizer (Molecular Devices, San  
591 Jose, CA, USA). To determine inhibitory tone onto respiratory motor neurons,  
592 bicuculline (50  $\mu\text{M}$ ) was focally applied using a Picospritzer II (General Valve  
593 Corporation, Fairfield, NJ, USA) to the recorded cell following a baseline period ( $\geq 10$   
594 respiratory bursts). Bicuculline was applied using a 5 sec pulse, every 10 secs for 5-10  
595 minutes with the picospritzer pipette slightly larger ( $\sim 2\text{ }\mu\text{m}$  diameter) than typical for  
596 focal application and placed approximately 15  $\mu\text{m}$  away from the cell body. This  
597 approach was taken to saturate the cell and surrounding area with the  $\text{GABA}_{\text{A}}$   
598 antagonist. Importantly, this approach did not recapitulate systemic effects of bicuculline  
599 on the vagal motor pool as the population spans nearly 2.5mm in the rostrocaudal axis  
600 in ranid frogs [55] and only a subset of the vagal motor pool was exposed in the  
601 preparation as described above. A washout period was used to verify changes in cell  
602 firing frequency were due to drug application and not cell drift. Most patched cells were

603 near the surface of the tissue as the thickness of the preparation hindered cell  
604 visualization. As a result, changes in firing frequency during bicuculline application and  
605 wash were rapid, suggesting the area was saturated with drug upon administration and  
606 then quickly washed. In a subset of cells where a gigaohm seal was not formed,  
607 recordings of action potentials were performed in the loose-patch configuration  
608 ( $V_{\text{hold}}=0$  mV;  $n=2$  in control, and  $n=2$  in hibernation). Regardless of recording  
609 configuration, firing rate data from recorded neurons were combined in group analysis  
610 of firing frequency, as data from loose-patch aligned with data from whole cell  
611 configuration. All voltages from current-clamp experiments were corrected for a liquid  
612 junction potential of 12 mV.

613

### 614 **Brain Slice electrophysiology**

615 Following dye labeling, in a subset of experiments brainstem slices (300  $\mu\text{m}$ ) containing  
616 labeled motor neurons were obtained ( $n=11$  bullfrogs). Whole-cell recordings were  
617 made from labeled motor neurons with an Axopatch 200B amplifier (Molecular Devices)  
618 in voltage clamp ( $V_{\text{hold}}=-60$  mV) mode. Glass pipettes (2.6-4 M $\Omega$ ) were filled with a  
619 solution containing (in mM): 95 CsCl, 2 MgCl<sub>2</sub>, 10 Hepes, 1 Na<sub>2</sub>-ATP, 0.1 Na<sub>2</sub>-GTP, 10  
620 EGTA, 1 CaCl<sub>2</sub> and 10 tetraethylammonium-Cl (TEA), pH  $\sim$  7.2 using CsOH. Data were  
621 acquired in pClamp 11 software using an Axopatch 200B amplifier and Axon Digidata  
622 1550B digitizer (Molecular Devices, San Jose, CA, USA). To examine miniature  
623 inhibitory postsynaptic currents (mIPSCs), tetrodotoxin (TTX; 250 nM) and DNQX (10  
624  $\mu\text{M}$ ) were bath applied for 3 min to block voltage-gated Na<sup>+</sup> channels and AMPA  
625 receptors. Strychnine (5  $\mu\text{M}$ ) was then bath applied in combination with TTX and DNQX  
626 for 2 min to block glycinergic mIPSCs and isolate GABAergic mIPSCs which were  
627 recorded for 1 min. All GABAergic mIPSCs were blocked following perfusion of  
628 bicuculline (50  $\mu\text{M}$ ) confirming their isolation. A 10 mV step was performed at the  
629 beginning of each recording and before each solution change to monitor series  
630 resistance ( $R_s$ ; estimated from the peak of the capacitive transient) and input resistance  
631 ( $R_{\text{IN}}$ ; estimated from the steady-state current).  $R_s$  was not compensated but remained  
632  $<25$  M $\Omega$  for inclusion.

633

### 634 **Data Analysis**

635 For experiments using the intact brainstem preparation, respiratory burst frequency was  
636 determined from integrated vagus nerve signals using the peak analysis function in  
637 LabChart 8 (ADInstruments Inc., Colorado Springs, CO, USA). Respiratory bursts were  
638 identified based on standard metrics used in the field such as  $\sim$ 1 s duration [56, 57].  
639 Burst start and stop time points were defined as 5% of the height from baseline. In  
640 experiments where muscimol was systemically applied, data were sampled from the last  
641 3 minutes of each condition (baseline, 500 nM, 1  $\mu\text{M}$ , and 3  $\mu\text{M}$ ). In experiments where  
642 bicuculline was systemically applied, data were sampled for 10 minutes during each  
643 condition (baseline, 500 nM, 1  $\mu\text{M}$ , 5  $\mu\text{M}$ , 10  $\mu\text{M}$ ). In systemic bicuculline experiments  
644 where non-respiratory bursting was quantified, non-respiratory were identified by their  
645 long duration and qualitatively different shape than respiratory bursts and were counted  
646 manually. Non-respiratory bursts appeared in a variety of output patterns as previously  
647 characterized *in vitro* (Reid and Milsom, 1998). Non-respiratory bursts were not  
648 quantified during systemic muscimol exposure as they were largely absent from

649 baseline recordings and only emerged with notable frequency following disinhibition with  
650 bicuculline. For temperature experiments, burst frequency was averaged in the last 5  
651 minutes at each temperature, and burst amplitudes were sampled in the last minute or  
652 in the case of the failure temperature, bursts were sampled directly before failure. To  
653 compare respiratory burst amplitudes in the cold, we analyzed the change from baseline  
654 at the coldest temperature the preparation could produce activity. Across control and  
655 hibernation groups this typically occurred at 8-10°C.

656

657 For experiments using the semi-intact preparation, action potentials were detected with  
658 the peak analysis function in LabChart 8 (ADInstruments Inc., Colorado Springs, CO,  
659 USA). Following detection of action potentials, a channel was created that plotted firing  
660 frequency over time. Average firing frequency per respiratory burst was determined via  
661 the mean firing frequency from neuronal burst start to stop. Average firing frequency  
662 was sampled and averaged from 10 respiratory bursts in each condition (baseline,  
663 bicuculline, and wash).

664

665 For voltage-clamp experiments in brainstem slices, average amplitude (current  
666 measurement from baseline to peak), charge transfer (integral of the mIPSC), rise time  
667 (time from baseline to peak), and frequency of GABAergic mIPSCs (mIPSC/sec) were  
668 analyzed from one minute of gap-free recording following two minutes of exposure to  
669 TTX/DNQX/Strychnine (as described above) using the peak analysis function in  
670 LabChart 8 (ADInstruments Inc., Colorado Springs, CO, USA). Events below 7.5 pA  
671 were excluded. Events were inspected manually to ensure the accurate detection of  
672 mIPSCs. For construction of the cumulative probability histogram, the first 50 mIPSCs  
673 from the minute of data obtained from each neuron were sampled.

674

## 675 **Statistics**

676 Data are presented as mean  $\pm$  s.d. unless otherwise stated or shown as individual  
677 points and means to highlight individual responses. When two groups of dependent  
678 samples were compared (“before-after” experiments), a two-tailed paired t-test was  
679 used. When two groups of independent samples were compared, a two-tailed unpaired  
680 t-test was used. Non-parametric versions of these tests were used if data sets were not  
681 normally distributed. In experiments with one main effect, a one-way ANOVA was used  
682 to test for the main effect and the interaction effect. One-way ANOVA was followed up  
683 with Holm-Sidak multiple comparisons test. In experiments with two main effects, a two-  
684 way ANOVA was used to test for the two main effects and the interaction effect. Two-  
685 way ANOVA was followed up with Holm-Sidak multiple comparisons test unless  
686 otherwise specified. Cumulative distributions were compared with the Kolmogorov-  
687 Smirnov test. Significance was accepted when  $P < 0.05$ . All analyses were performed  
688 using GraphPad Prism (v9.4.1, San Diego, CA, USA).

689

690

## 691 **Declarations**

692

693 Ethics approval and consent to participate: Animal experiments were approved by  
694 University of Missouri Animal Care and Use Committee protocol #39264

- 695
- Consent for publication: The authors each consent to the publication of this work.
- 696
- Availability of data and materials: Data will be made available upon request.
- 697
- Competing interests: Santin is a Guest Editor of the Special Issue “Synaptic
- 698
- plasticity, learning, and memory” at *BMC Biology*. The authors have no other
- 699
- competing interests to declare.
- 700
- Funding: National Institutes of Health R01NS114514 to JS
- 701
- Authors' contributions: Conceived research; JS, SS. Designed research; JS, SS.
- 702
- Performed experiments; SS. Analyzed data; SS, JS. Drafted original manuscript;
- 703
- SS, JS. Edited, revised, and finalized manuscript; SS, JS
- 704
- Acknowledgements: The authors would like to thank Dr. Joe Viteri for comments
- 705
- on a previous version of this manuscript.
- 706
- 707
- 708
- 709
- 710
- 711
- 712
- 713
- 714
- 715
- 716
- 717
- 718
- 719
- 720
- 721
- 722
- 723
- 724
- 725
- 726

727 **References:**

- 728 1. Marom S, Marder E: **A biophysical perspective on the resilience of neuronal**  
729 **excitability across timescales.** *Nature Reviews Neuroscience* 2023,  
730 **24(10):640-652.**
- 731 2. Desai NS, Rutherford LC, Turrigiano GG: **Plasticity in the intrinsic excitability**  
732 **of cortical pyramidal neurons.** *Nature neuroscience* 1999, **2(6):515-520.**
- 733 3. Kilman V, Van Rossum MC, Turrigiano GG: **Activity deprivation reduces**  
734 **miniature IPSC amplitude by decreasing the number of postsynaptic**  
735 **GABAA receptors clustered at neocortical synapses.** *Journal of*  
736 *Neuroscience* 2002, **22(4):1328-1337.**
- 737 4. Turrigiano GG, Leslie KR, Desai NS, Rutherford LC, Nelson SB: **Activity-**  
738 **dependent scaling of quantal amplitude in neocortical neurons.** *Nature*  
739 1998, **391(6670):892-896.**
- 740 5. Davis GW, DiAntonio A, Petersen SA, Goodman CS: **Postsynaptic PKA**  
741 **controls quantal size and reveals a retrograde signal that regulates**  
742 **presynaptic transmitter release in Drosophila.** *Neuron* 1998, **20(2):305-315.**
- 743 6. LeMasson G, Marder E, Abbott L: **Activity-dependent regulation of**  
744 **conductances in model neurons.** *Science* 1993, **259(5103):1915-1917.**
- 745 7. Barnes SJ, Franzoni E, Jacobsen RI, Erdelyi F, Szabo G, Clopath C, Keller GB,  
746 Keck T: **Deprivation-induced homeostatic spine scaling in vivo is localized**  
747 **to dendritic branches that have undergone recent spine loss.** *Neuron* 2017,  
748 **96(4):871-882. e875.**
- 749 8. Hengen KB, Lambo ME, Van Hooser SD, Katz DB, Turrigiano GG: **Firing rate**  
750 **homeostasis in visual cortex of freely behaving rodents.** *Neuron* 2013,  
751 **80(2):335-342.**
- 752 9. Ransdell JL, Nair SS, Schulz DJ: **Rapid homeostatic plasticity of intrinsic**  
753 **excitability in a central pattern generator network stabilizes functional**  
754 **neural network output.** *The Journal of Neuroscience* 2012, **32(28):9649-9658.**
- 755 10. Gainey MA, Aman JW, Feldman DE: **Rapid disinhibition by adjustment of PV**  
756 **intrinsic excitability during whisker map plasticity in mouse S1.** *Journal of*  
757 *Neuroscience* 2018, **38(20):4749-4761.**
- 758 11. Kuhlman SJ, Olivas ND, Tring E, Ikrar T, Xu X, Trachtenberg JT: **A disinhibitory**  
759 **microcircuit initiates critical-period plasticity in the visual cortex.** *Nature*  
760 2013, **501(7468):543-546.**
- 761 12. Wu C-H, Ramos R, Katz DB, Turrigiano GG: **Homeostatic synaptic scaling**  
762 **establishes the specificity of an associative memory.** *Current biology* 2021,  
763 **31(11):2274-2285. e2275.**
- 764 13. Marder E, Rue MC: **From the neuroscience of individual variability to climate**  
765 **change.** *Journal of Neuroscience* 2021, **41(50):10213-10221.**
- 766 14. Tattersall GJ, Ultsch GR: **Physiological ecology of aquatic overwintering in**  
767 **ranid frogs.** *Biological Reviews* 2008, **83(2):119-140.**
- 768 15. Santin JM, Hartzler LK: **Activation of respiratory muscles does not occur**  
769 **during cold-submergence in bullfrogs, Lithobates catesbeianus.** *Journal of*  
770 *Experimental Biology* 2017, **220(7):1181-1186.**



- 771 16. Santin JM, Vallejo M, Hartzler LK: **Synaptic up-scaling preserves motor circuit**  
772 **output after chronic, natural inactivity.** *eLife* 2017, **6**.
- 773 17. Zubov T, do Amaral-Silva L, Santin JM: **Inactivity and Ca<sup>2+</sup> signaling regulate**  
774 **synaptic compensation in motoneurons following hibernation in American**  
775 **bullfrogs.** *Scientific Reports* 2022, **12**(1):1-13.
- 776 18. Amaral-Silva L, Santin JM: **Synaptic modifications transform neural networks**  
777 **to function without oxygen.** *BMC Biology* 2023, **Accepted for publication**.
- 778 19. Bueschke N, do Amaral-Silva L, Adams S, Santin JM: **Transforming a neural**  
779 **circuit to function without oxygen and glucose delivery.** *Current Biology*  
780 2021, **31**(24):R1564-R1565.
- 781 20. Rue MC, Alonso LM, Marder E: **Repeated applications of high potassium**  
782 **elicit long-term changes in a motor circuit from the crab, *Cancer borealis*.**  
783 *Iscience* 2022, **25**(9).
- 784 21. Alonso LM, Rue MC, Marder E: **Gating of homeostatic regulation of intrinsic**  
785 **excitability produces cryptic long-term storage of prior perturbations.**  
786 *Proceedings of the National Academy of Sciences* 2023, **120**(26):e2222016120.
- 787 22. Arendt KL, Sarti F, Chen L: **Chronic inactivation of a neural circuit enhances**  
788 **LTP by inducing silent synapse formation.** *Journal of Neuroscience* 2013,  
789 **33**(5):2087-2096.
- 790 23. Mitra A, Mitra SS, Tsien RW: **Heterogeneous reallocation of presynaptic**  
791 **efficacy in recurrent excitatory circuits adapting to inactivity.** *Nature*  
792 *neuroscience* 2012, **15**(2):250-257.
- 793 24. Broch L, Morales RD, Sandoval AV, Hedrick MS: **Regulation of the respiratory**  
794 **central pattern generator by chloride-dependent inhibition during**  
795 **development in the bullfrog (*Rana catesbeiana*).** *Journal of Experimental*  
796 *Biology* 2002, **205**(8):1161-1169.
- 797 25. Wright AH: **North American anura: life-histories of the anura of Ithaca, New**  
798 **York:** Carnegie institution of Washington; 1914.
- 799 26. Willis YL, Moyle DL, Baskett TS: **Emergence, breeding, hibernation,**  
800 **movements and transformation of the bullfrog, *Rana catesbeiana*, in**  
801 **Missouri.** *Copeia* 1956:30-41.
- 802 27. Kottick A, Baghdadwala MI, Ferguson EV, Wilson RJ: **Transmission of the**  
803 **respiratory rhythm to trigeminal and hypoglossal motor neurons in the**  
804 **American Bullfrog (*Lithobates catesbeiana*).** *Respiratory physiology*  
805 *& neurobiology* 2013, **188**(2):180-191.
- 806 28. Kinkead R: **Phylogenetic trends in respiratory rhythmogenesis: insights**  
807 **from ectothermic vertebrates.** *Respiratory physiology & neurobiology* 2009,  
808 **168**(1):39-48.
- 809 29. Milsom W, Reid S, Meier J, Kinkead R: **Central respiratory pattern generation**  
810 **in the bullfrog, *Rana catesbeiana*.** *Comparative Biochemistry and Physiology*  
811 *Part A: Molecular & Integrative Physiology* 1999, **124**(3):253-264.
- 812 30. Reid SG, Milsom WK: **Respiratory pattern formation in the isolated bullfrog**  
813 **(*Rana catesbeiana*) brainstem-spinal cord.** *Respiration physiology* 1998,  
814 **114**(3):239-255.



- 815 31. Saunders SE, Santin JM: **Activation of respiratory-related bursting in an**  
816 **isolated medullary section from adult bullfrogs.** *Journal of Experimental*  
817 *Biology* 2023, **226**(18).
- 818 32. Martinez D, Santin JM, Schulz D, Nadim F: **The differential contribution of**  
819 **pacemaker neurons to synaptic transmission in the pyloric network of the**  
820 **Jonah crab, *Cancer borealis*.** *Journal of neurophysiology* 2019, **122**(4):1623-  
821 1633.
- 822 33. Swensen AM, Golowasch J, Christie AE, Coleman MJ, Nusbaum MP, Marder E:  
823 **GABA and responses to GABA in the stomatogastric ganglion of the crab**  
824 ***Cancer borealis*.** *Journal of Experimental Biology* 2000, **203**(14):2075-2092.
- 825 34. Amaral-Silva L, Santin JM: **A brainstem preparation allowing simultaneous**  
826 **access to respiratory motor output and cellular properties of motoneurons**  
827 **in American bullfrog.** *Journal of Experimental Biology* 2022.
- 828 35. Santin JM, Hartzler LK: **Control of lung ventilation following overwintering**  
829 **conditions in bullfrogs, *Lithobates catesbeianus*.** *Journal of Experimental*  
830 *Biology* 2016, In press, doi:10.1242/jeb.136259.
- 831 36. Gottlieb G, Jackson DC: **Importance of pulmonary ventilation in respiratory**  
832 **control in the bullfrog.** *Am J Physiol* 1976, **230**(3):608-613.
- 833 37. Morales RD, Hedrick MS: **Temperature and pH/CO<sub>2</sub> modulate respiratory**  
834 **activity in the isolated brainstem of the bullfrog *Rana catesbeiana*.** *Comp*  
835 *Biochem Physiol- A Mol Int Physiol* 2002, **132**(2):477-487.
- 836 38. Fournier S, Allard M, Roussin S, Kinkead R: **Developmental changes in central**  
837 **O<sub>2</sub> chemoreflex in *Rana catesbeiana*: the role of noradrenergic modulation.**  
838 *Journal of Experimental Biology* 2007, **210**(17):3015-3026.
- 839 39. Vallejo M, Santin JM, Hartzler LK: **Noradrenergic modulation determines**  
840 **respiratory network activity during temperature changes in the in vitro**  
841 **brainstem of bullfrogs.** *Respiratory physiology & neurobiology* 2018, **258**:25-  
842 31.
- 843 40. Kam K, Worrell JW, Janczewski WA, Cui Y, Feldman JL: **Distinct inspiratory**  
844 **rhythm and pattern generating mechanisms in the preBötzinger complex.**  
845 *Journal of Neuroscience* 2013, **33**(22):9235-9245.
- 846 41. Del Negro CA, Funk GD, Feldman JL: **Breathing matters.** *Nat Rev Neurosci*  
847 2018.
- 848 42. Santin JM, Hartzler LK: **Environmentally-induced return to juvenile-like**  
849 **chemosensitivity in the respiratory control system of adult bullfrogs,**  
850 ***Lithobates catesbeianus*.** *The Journal of Physiology* 2016.
- 851 43. Burggren WW: **Phenotypic switching resulting from developmental**  
852 **plasticity: fixed or reversible?** *Frontiers in Physiology* 2020, **10**:1634.
- 853 44. Santin J, Hartzler L: **Temperature influences CO<sub>2</sub>/pH-sensitivity in locus**  
854 **coeruleus neurons of the bullfrog, *Lithobates catesbeianus*.** *FASEB J* 2013,  
855 **27**(714.12).
- 856 45. Amaral-Silva L, Santin JM: **Molecular profiling of CO<sub>2</sub>/pH-sensitive neurons**  
857 **in the locus coeruleus of bullfrogs reveals overlapping noradrenergic and**  
858 **glutamatergic cell identity.** *Comparative Biochemistry and Physiology Part A:*  
859 *Molecular & Integrative Physiology* 2023, **283**:111453.

- 860 46. Turrigiano G, LeMasson G, Marder E: **Selective regulation of current densities**  
861 **underlies spontaneous changes in the activity of cultured neurons.** *Journal*  
862 *of Neuroscience* 1995, **15**(5):3640-3652.
- 863 47. Bueschke N, Amaral-Silva L, Hu M, Alvarez A, Santin JM: **Plasticity in the**  
864 **functional properties of NMDA receptors improves network stability during**  
865 **severe energy stress.** *The Journal of Neuroscience* 2024, **44**.
- 866 48. Marder E: **Individual variability, statistics, and the resilience of nervous**  
867 **systems of crabs and humans to temperature and other perturbations.**  
868 *Eneuro* 2023, **10**(11).
- 869 49. Chesler M: **Regulation and modulation of pH in the brain.** *Physiological*  
870 *reviews* 2003, **83**(4):1183-1221.
- 871 50. Haley JA, Hampton D, Marder E: **Two central pattern generators from the**  
872 **crab, *Cancer borealis*, respond robustly and differentially to extreme**  
873 **extracellular pH.** *eLife* 2018, **7**:e41877.
- 874 51. Brockhaus J, Ballanyi K: **Anticonvulsant A1 receptor-mediated adenosine**  
875 **action on neuronal networks in the brainstem–spinal cord of newborn rats.**  
876 *Neuroscience* 2000, **96**(2):359-371.
- 877 52. Matesz C, Szekely G: **Organization of the ambiguous nucleus in the frog**  
878 **(*Rana esculenta*).** *Journal of Comparative Neurology* 1996, **371**(2):258-269.
- 879 53. McLean H, Kimura N, Kogo N, Perry SF, Remmers JE: **Fictive respiratory**  
880 **rhythm in the isolated brainstem of frogs.** *Journal of Comparative Physiology*  
881 *A* 1995, **176**(5):703-713.
- 882 54. Kogo N, Remmers JE: **Neural organization of the ventilatory activity in the**  
883 **frog, *Rana catesbeiana*. II.** *Journal of neurobiology* 1994, **25**(9):1080-1094.
- 884 55. Stuesse SL, Cruce WL, Powell KS: **Organization within the cranial IX–X**  
885 **complex in ranid frogs: a horseradish peroxidase transport study.** *Journal*  
886 *of Comparative Neurology* 1984, **222**(3):358-365.
- 887 56. Winmill RE, Chen AK, Hedrick MS: **Development of the respiratory response**  
888 **to hypoxia in the isolated brainstem of the bullfrog *Rana catesbeiana*.**  
889 *Journal of experimental biology* 2005, **208**(2):213-222.
- 890 57. Kogo N, Perry SF, Remmers JE: **Neural organization of the ventilatory**  
891 **activity in the frog, *Rana catesbeiana*. I.** *Journal of neurobiology* 1994,  
892 **25**(9):1067-1079.

893

894

895

896

897

898

899

900

901 **Figures Legends:**

902 **Fig. 1 GABAergic tone that controls respiratory burst frequency strongly**  
903 **decreases following hibernation.** Integrated vagus nerve activity (CN X) was rhythmic  
904 in fully intact brainstem preparations (top right box) from control and hibernated animals.  
905 A) Top, continuous recording of CNX during perfusion of increasing doses of bicuculline  
906 in a control preparation (black). Bottom, zoomed in view of epochs (orange boxes)  
907 indicated in continuous trace directly above. In control preparations, bath application of  
908 bicuculline led to a dose dependent decrease in respiratory burst frequency and dose-  
909 dependent increase in non-respiratory burst frequency. B) Top, continuous recording of  
910 CNX during perfusion of increasing doses of bicuculline in a preparation from a  
911 hibernated animal (blue). Bottom, zoomed in view of epochs (orange boxes) indicated in  
912 continuous trace above. Respiratory output from hibernated preparations was  
913 insensitive to systemic application of bicuculline, however non-respiratory motor  
914 bursting increased in a dose-dependent manner like controls. C) Summary of  
915 bicuculline-mediated changes in respiratory burst frequency. There was a significant  
916 interaction between drug and group by two-way ANOVA ( $F_{(4,32)}=6.741$ ;  $p=0.0005$ ).  
917 Additionally, at 10  $\mu\text{M}$  bicuculline, respiratory burst frequency from controls was  
918 significantly lower than hibernated preparations by Holm-Sidak's post-hoc test  
919 ( $p=0.0111$ ;  $n=5/\text{group}$ ). D) Summary of bicuculline-mediated changes in non-respiratory  
920 burst frequency. Bicuculline mediated similar increases in non-respiratory bursting in  
921 control and hibernated groups. There was no significant interaction between drug and  
922 group by two-way ANOVA ( $F_{(4,32)}=0.7948$ ;  $p=0.5373$ ;  $n=5/\text{group}$ ). a.u., arbitrary units. In  
923 summary plots, thick lines represent the group average and thin lines are responses of  
924 individual preparations.

925  
926 **Fig. 2 Hibernation decreases sensitivity to GABA<sub>A</sub>R agonist (muscimol)-mediated**  
927 **respiratory frequency decline.** Integrated vagus nerve activity (CN X) was rhythmic in  
928 fully intact brainstem preparations (top left box) from control and hibernated animals. A)  
929 Continuous recording of CNX during perfusion of increasing doses of muscimol in a  
930 control preparation (black). In control preparations, respiratory output was unchanged  
931 by bath application of 500nM muscimol but decreased following elevation to 1 $\mu\text{M}$   
932 muscimol and ultimately stopped following further elevation to 3 $\mu\text{M}$  muscimol.  
933 Preparations were recovered by exposure to bicuculline, demonstrating specificity of the  
934 GABA<sub>A</sub> receptor agonist. B) Continuous recording of CNX during perfusion of increasing  
935 doses of muscimol in a preparation from a hibernated animal (blue). Preparations from  
936 hibernated animals were relatively insensitive to muscimol mediated changes in  
937 respiratory burst frequency compared to controls. C) Summary of muscimol-mediated  
938 changes in respiratory burst frequency. There was a significant interaction between drug  
939 and group by two-way ANOVA ( $F_{(3,24)}=4.045$ ;  $p=0.0184$ ). Additionally, at 1  $\mu\text{M}$  muscimol,  
940 respiratory burst frequency from controls was significantly lower than hibernated  
941 preparations by Holm-Šidák's post-hoc test ( $p=0.0007$ ,  $n=5/\text{group}$ ). D) Summary of  
942 muscimol-mediated changes in respiratory burst frequency relative to baseline. There  
943 was a significant interaction between drug and group by two-way ANOVA ( $F_{(3,24)}=7.184$ ;  
944  $p=0.0013$ ). Additionally, at 1  $\mu\text{M}$  muscimol, respiratory burst frequency from controls

945 was significantly lower than hibernated preparations relative to baseline by Holm-  
946 Sidak's post-hoc test ( $p=0.0030$ ,  $n=5$  per group). In summary plots, thick lines represent  
947 the group average and thin lines are individual preparations.

948 **Fig. 3 Postsynaptic GABAergic currents in motoneurons are unchanged following**  
949 **hibernation.** A) Example voltage clamp traces of GABAergic miniature inhibitory  
950 postsynaptic currents (mIPSCs; holding potential =  $-60$  mV;  $250$  nM TTX,  $10$   $\mu$ M DNQX,  
951  $5$   $\mu$ M strychnine) from control (black) and hibernated (blue) identified vagal motor  
952 neurons in brain slice (middle right box). Addition of  $50$   $\mu$ M bicuculline (Bic) to the bath  
953 eliminated mIPSCs in both groups, confirming GABAergic identity. B) Cumulative  
954 probability histograms of mIPSC amplitudes from control neurons (black line),  
955 hibernated neurons (blue line) appeared nearly identical. Accordingly, there was no  
956 statistical difference between distributions from control and hibernated cells by  
957 Kolmogorov-Smirnov test ( $p = 0.5041$ ). C) Summary data. There was no statistical  
958 difference in mIPSC frequency, average amplitude, rise time, charge transfer, and  
959 neuronal input resistance by unpaired t-test ( $p > 0.05$ ;  $n = 16$  control cells;  $n=16$   
960 hibernated cells). Error bars are standard deviation (SD).

961

962 **Fig. 4 Hibernation decreases the influence of presynaptic GABA on motoneuron**  
963 **firing.** A) Integrated network output recorded on the trigeminal nerve (CN V) and  
964 simultaneous whole-cell current clamp recordings of vagal motor neurons (CN X MN)  
965 driven by the respiratory circuit in the semi-intact brainstem preparation (top left box). A  
966 pipette was used to focally apply bicuculline onto the recorded vagal motor neuron to  
967 isolate the GABAergic tone on individual neurons. An example respiratory neuron (CN X  
968 MN, gray, top right) fired rhythmic bursts, characterized by transient increases in firing  
969 frequency (Firing Freq, light gray, middle top right) during respiratory motor output  
970 (Black, bottom top right, CN V). B) Example respiratory motor activity in a control  
971 preparation (black). Example vagal motor neuron (CN X MN) fires bursts of action  
972 potentials during the respiratory burst (CN V). Focal application of bicuculline (gray box)  
973 to the motor neuron increases neuronal burst firing frequency (Firing Freq). C) Example  
974 respiratory motor activity in a preparation from a hibernated animal (blue). Example  
975 vagal motor neuron (CN X MN) also fired bursts of action potentials during the  
976 respiratory burst (CN V). Focal application of bicuculline (gray box) to the motor neuron  
977 increased neuronal burst firing frequency (Firing Freq,  $\Delta \sim 47$ Hz), but not to the same  
978 extent as the control neuron (Firing Freq,  $\Delta \sim 74$ Hz). D) Summary of bicuculline-mediated  
979 increases in motor neuron firing frequency. There was a significant interaction between  
980 drug and group by two-way ANOVA ( $F_{(2,38)}=6.391$ ;  $p=0.0041$ ). Furthermore, there was a  
981 significant increase in burst firing frequency following focal application of bicuculline in  
982 control but not hibernated cells by Holm-Sidak's post-hoc test ( $***p<0.0001$ ;  $n = 12$   
983 control cells;  $n=9$  hibernated cells). E) Summary of bicuculline-mediated fold change in  
984 burst firing frequency from baseline. Control cells had a significantly larger bicuculline-  
985 mediated fold change in burst firing frequency than hibernated cells by unpaired t-test  
986 ( $p=0.036$ ;  $n = 12$  control cells;  $n=9$  hibernated cells). Orange cells were recorded in

987 loose-patch configuration. Box plots represent interquartile range and whiskers  
988 represent the minimum to maximum values. a.u., arbitrary units. Error bars are  
989 standard deviation (SD).

990 **Fig. 5 Respiratory burst morphology after hibernation closely matches controls at**  
991 **room temperature.** Integrated vagus motor bursts (CN X) in preparations from 5  
992 controls (red) and 5 hibernators (blue). Overlaid bursts (n=50) from individual  
993 preparations are represented in different shades from top to bottom. Overlaying all  
994 bursts from all animals from both groups demonstrates a close matching between  
995 controls and hibernators, indicating the loss of GABA<sub>A</sub> receptors has no obvious impact  
996 on motor burst morphology after hibernation.

997

998 **Fig. 6 Lowering GABA<sub>A</sub>R signaling enhances motor performance of breathing at**  
999 **cold temperatures.** Integrated vagus nerve activity (CN X) from intact brainstem  
1000 preparations (bottom right box) showing the response of control (A, black), hibernators  
1001 (B, blue), and controls treated with 2 μM bicuculline (C, gray) during cooling ramps from  
1002 20°C to 8°C. Zoomed-in traces below the compressed recordings illustrate the effects of  
1003 cooling on burst amplitude. Arrows indicate the temperature at 50% of baseline burst  
1004 frequency. (D) Mean data showing average temperature responses of normalized burst  
1005 frequency among groups (two-way ANOVA interaction of group x temperature,  
1006 p<0.0001). (E) Mean data showing a significant difference in the temperature at 50% of  
1007 baseline burst rate between control, hibernators, and controls+bicuculline (one-way  
1008 ANOVA; p<0.0001) (F) Mean data showing change in burst amplitude from baseline in  
1009 control and hibernators during temperature changes. Controls undergo a decrease in  
1010 burst amplitude during cooling, while hibernators and controls+bicuculline maintain burst  
1011 amplitude throughout the cooling ramp (two-way ANOVA, p=0.0001 group x  
1012 temperature interaction); \* represents p<0.05, \*\*<0.01, \*\*\*<0.001 in Holm-Sidak multiple  
1013 comparisons test following one or two-way ANOVAs.

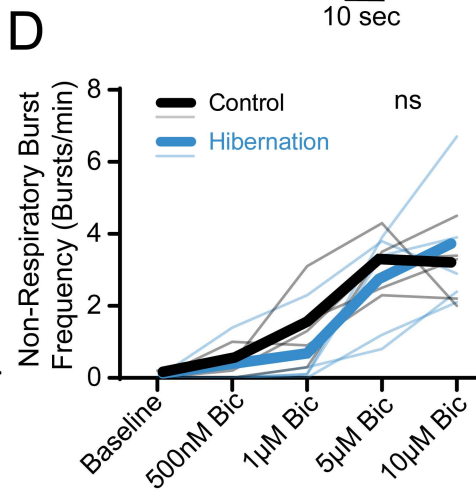
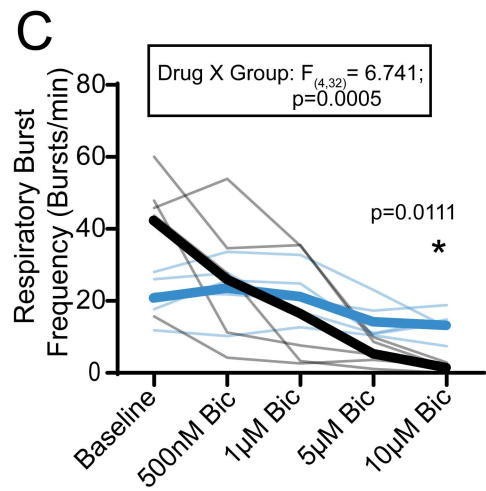
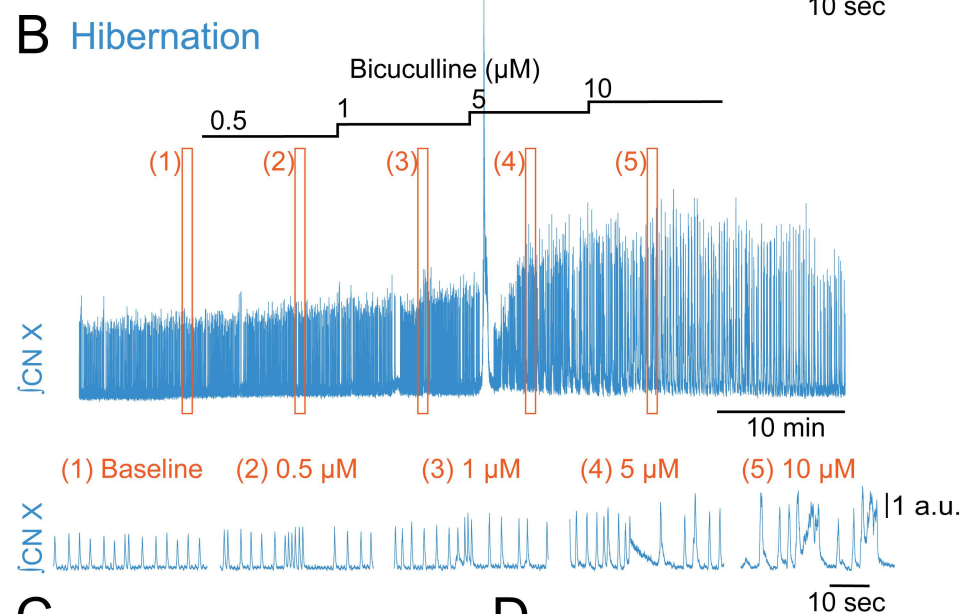
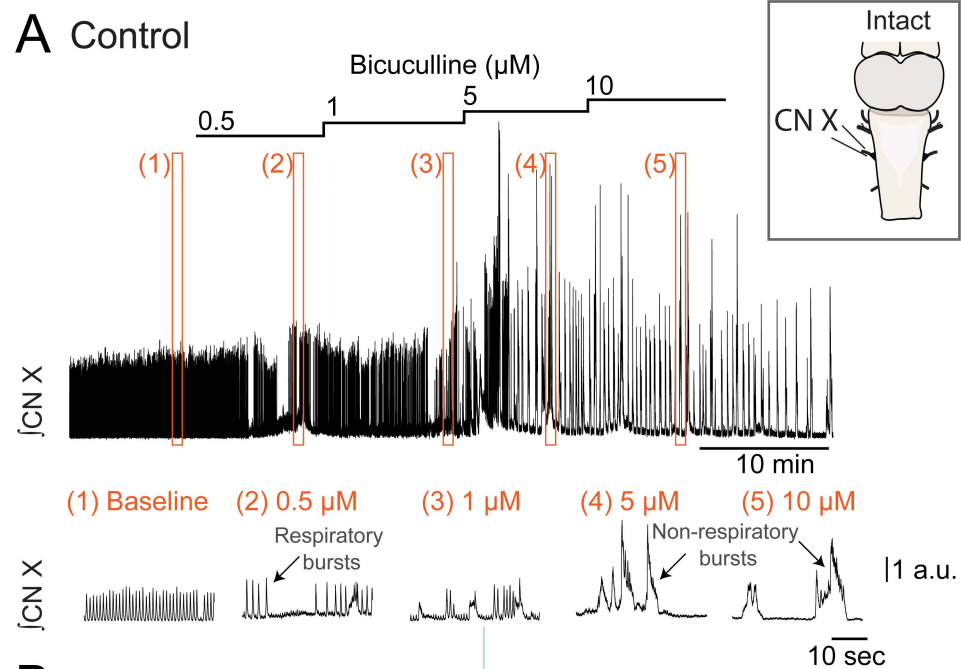
1014

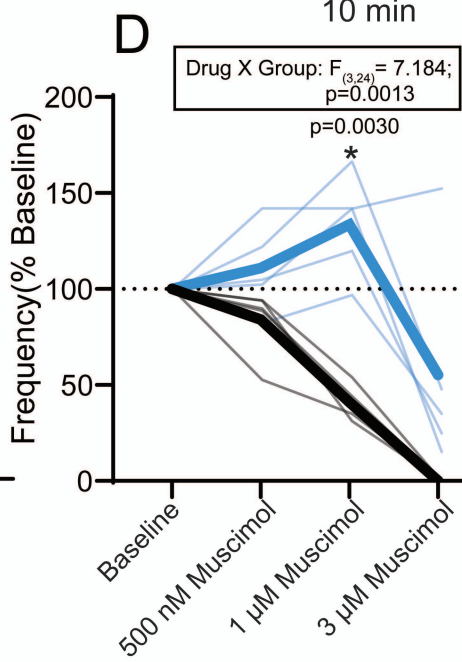
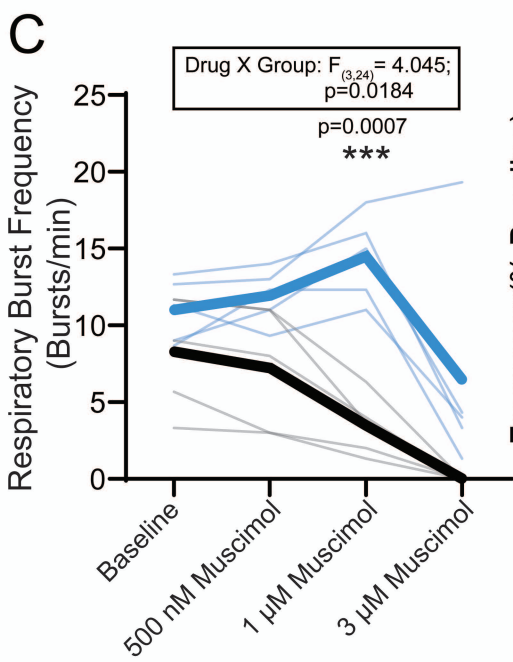
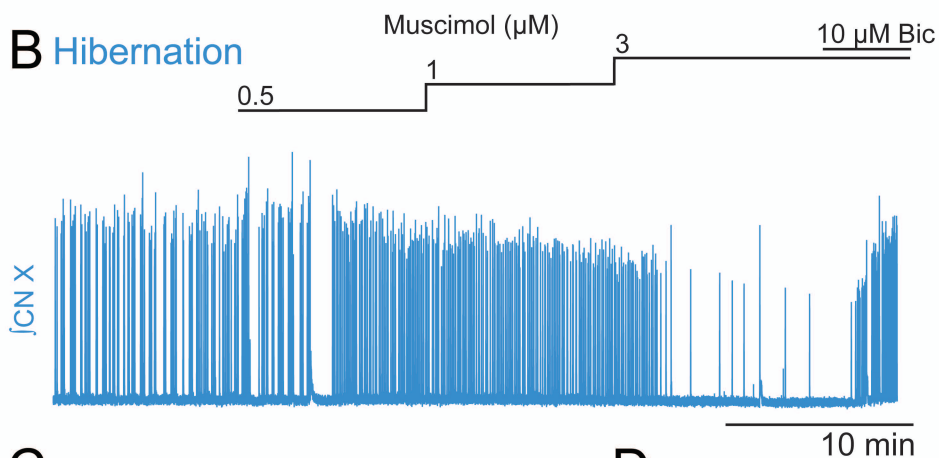
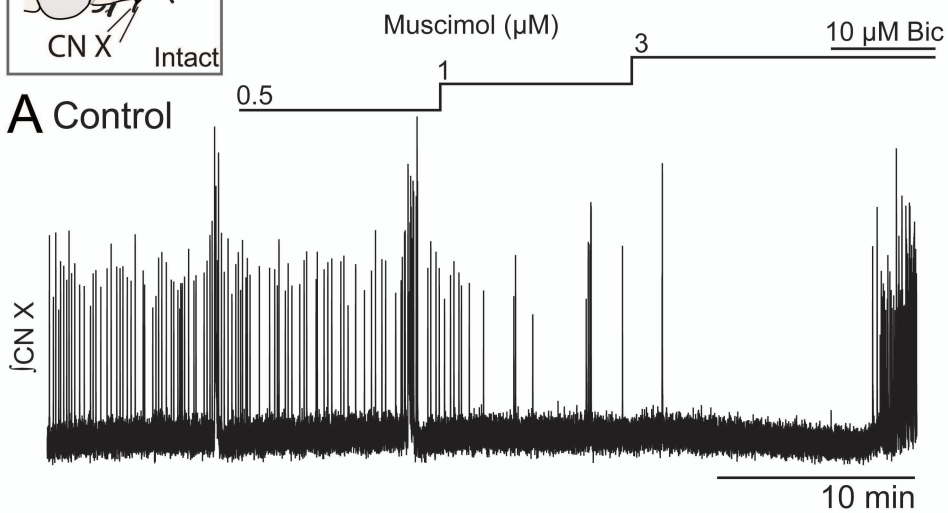
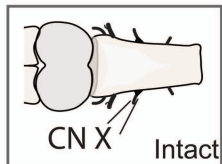
1015 **Fig. 7 Schematic illustrating how reducing inhibition may promote breathing in**  
1016 **the cold.** In controls at warm temperatures (orange left), inhibition (red, minus symbol)  
1017 plays an important role in generating the respiratory rhythm (circular arrows) and  
1018 controlling the excitability to motoneurons. Following hibernation (orange right), the  
1019 respiratory network decreases reliance on inhibition and potentially increases reliance  
1020 on mechanisms that involve excitation (dark blue, plus symbol) for respiratory  
1021 rhythmogenesis (circular arrows). Nonetheless, there is no discernable change in  
1022 network motor output at warm temperatures following hibernation compared to controls.  
1023 During acute cooling, inhibitory neurotransmission also plays a modulatory role and is  
1024 increased. As a result, controls (blue left) have marked reduction in respiratory  
1025 frequency and motor output at colder temperatures due to elevated GABAergic  
1026 inhibition. In contrast, output following hibernation is resistant to depressive effects of

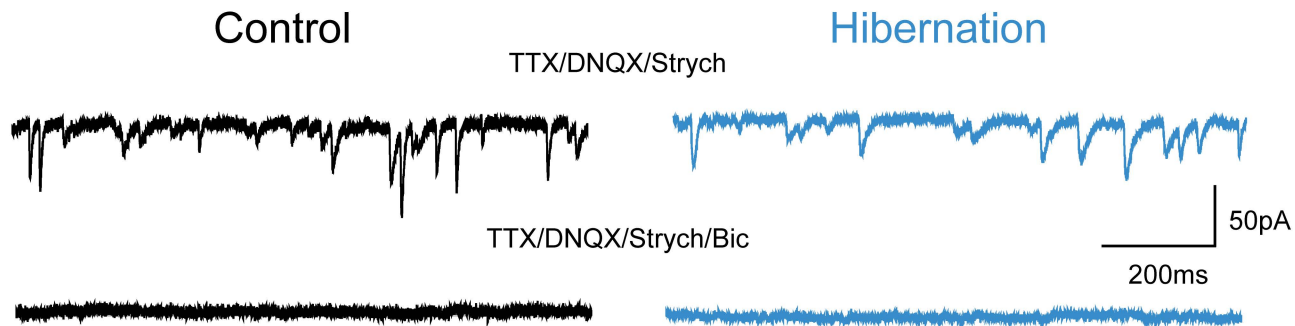
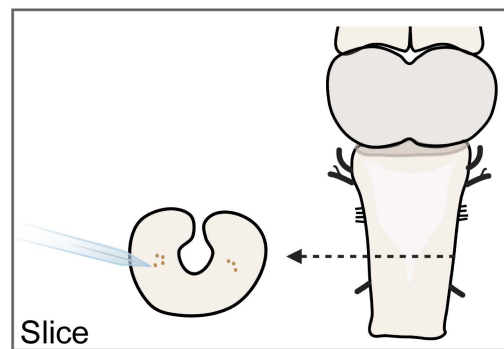
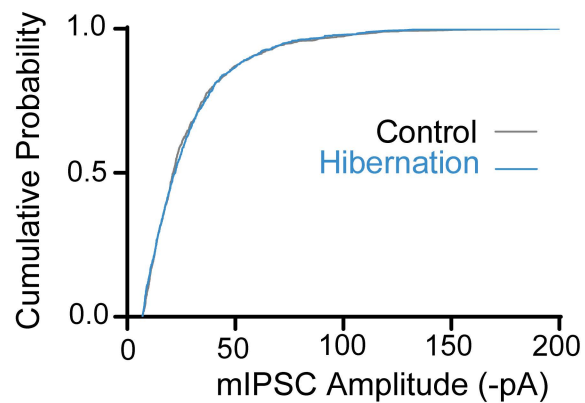
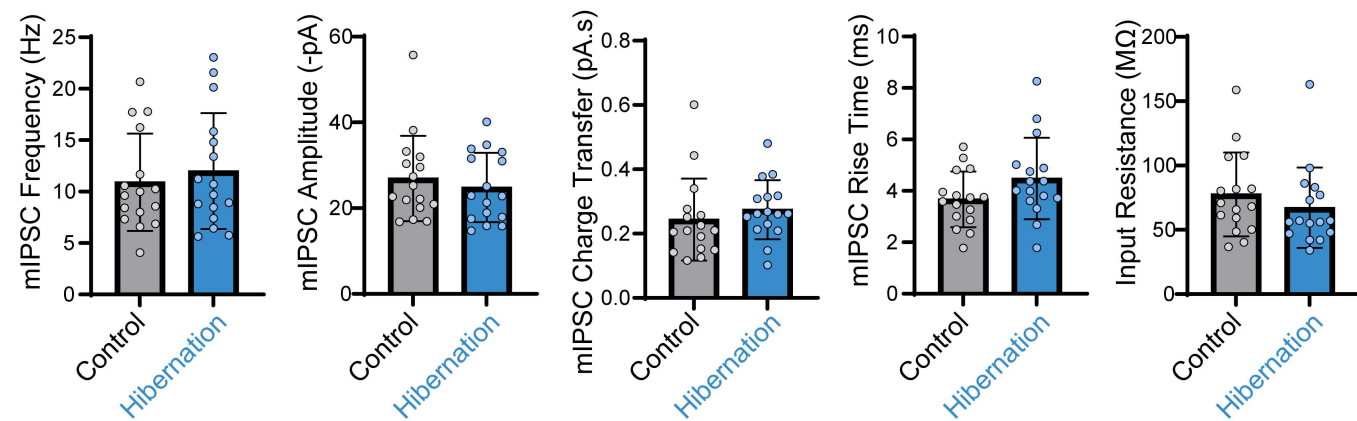


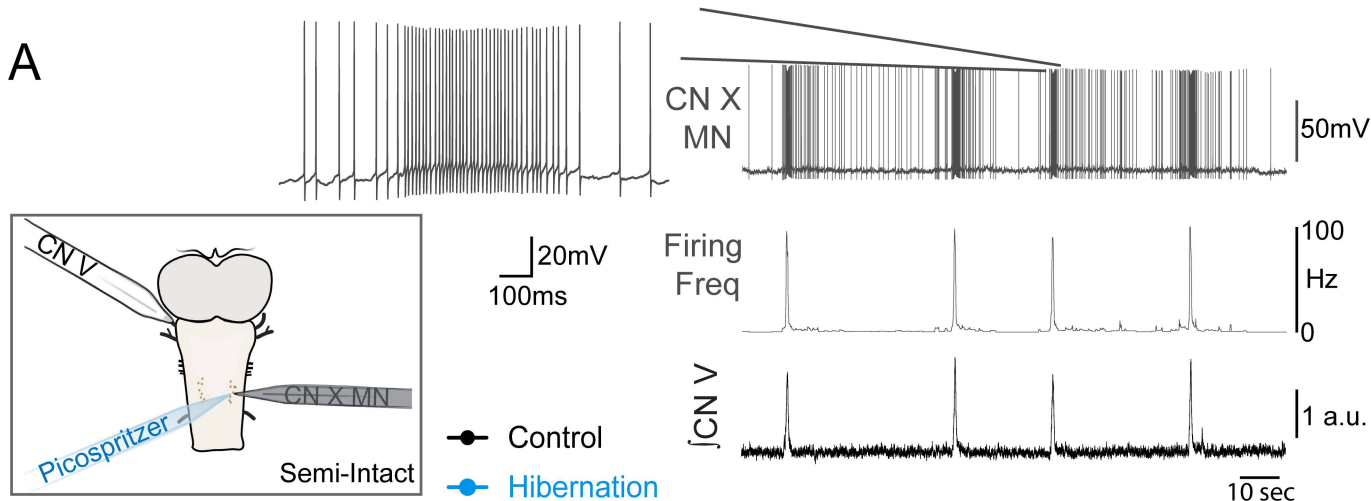
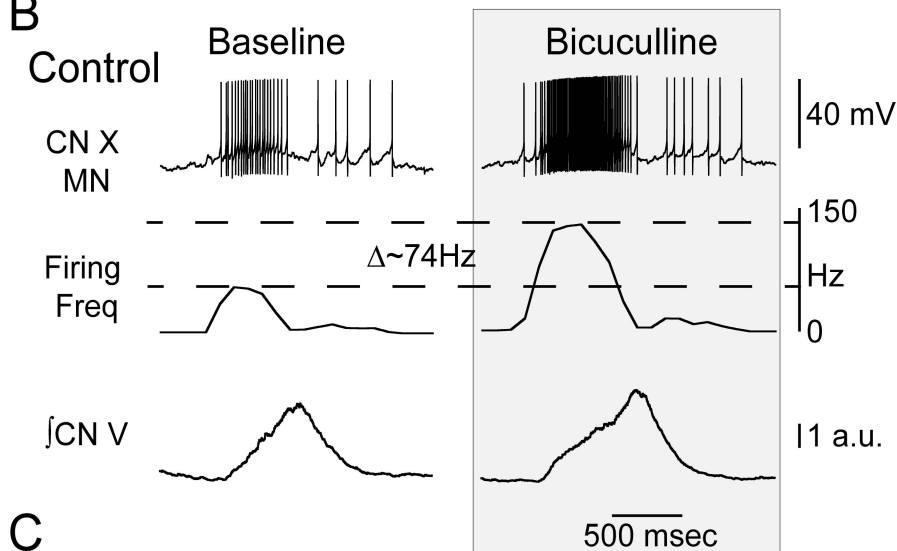
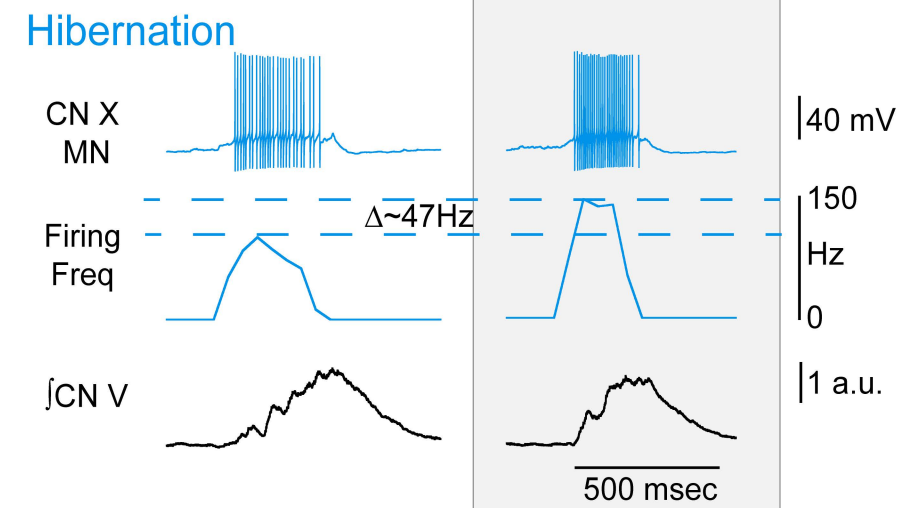
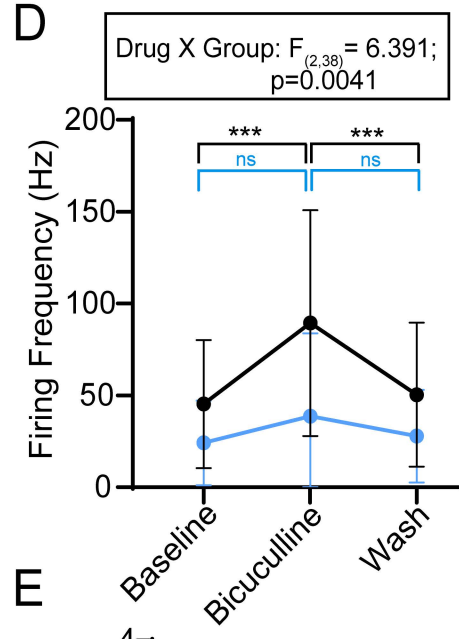
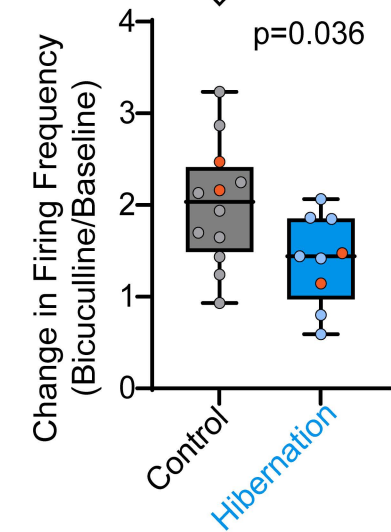
1027 the cold, likely with a contribution resulting from the decreased reliance on inhibition that  
1028 normally slows activity and depresses motor output. Thus, output following hibernation  
1029 is more robust at cooler temperatures, in part, because inhibitory neurotransmission is  
1030 decreased in rhythm-generating and interneuronal pathways.





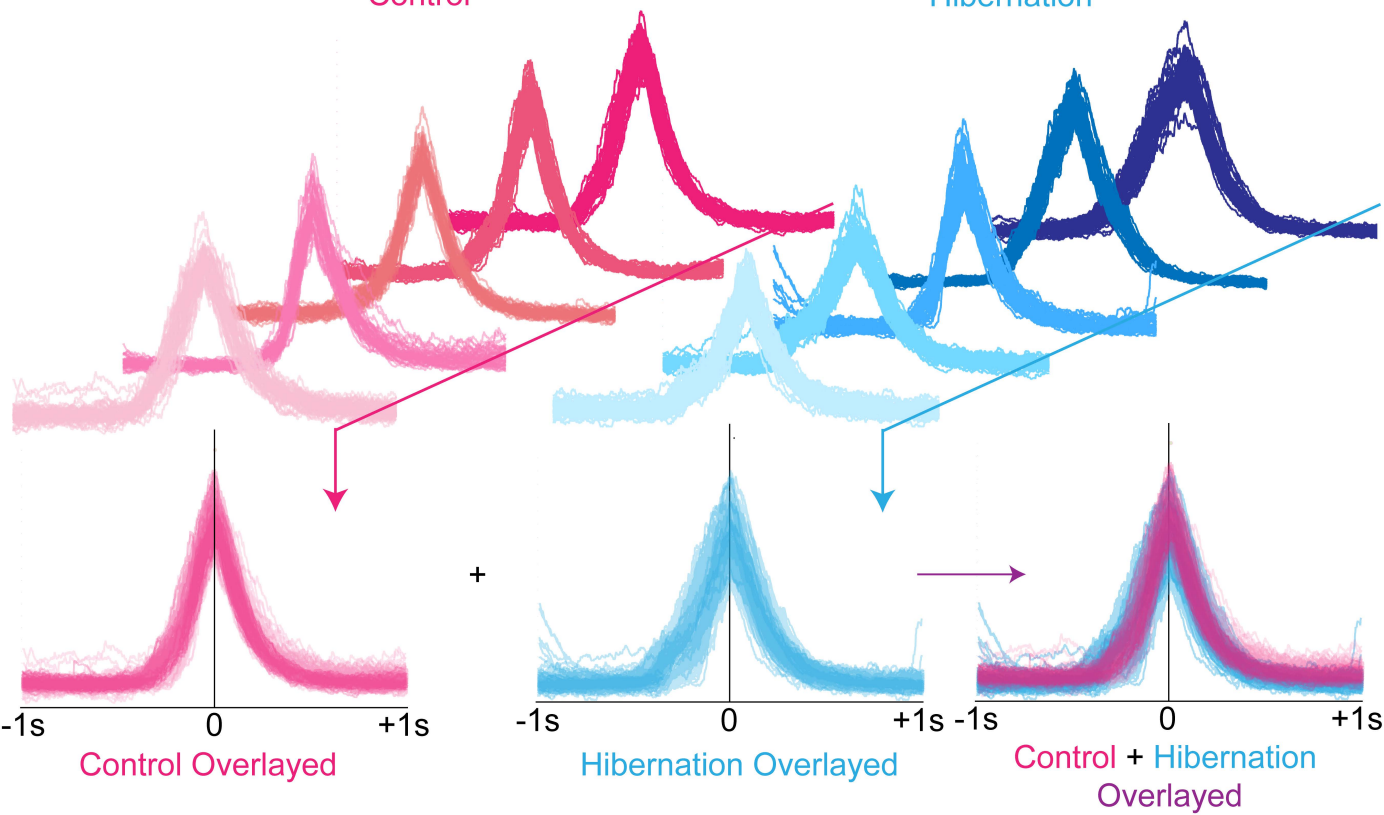


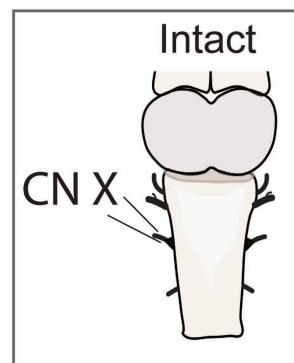
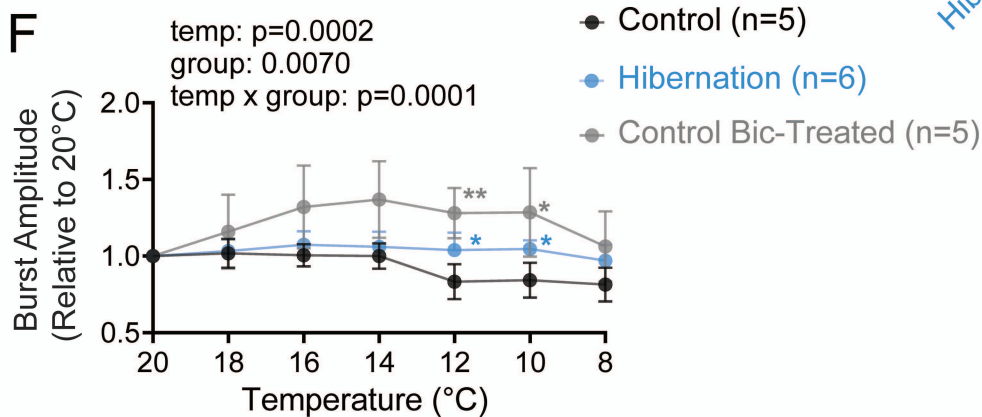
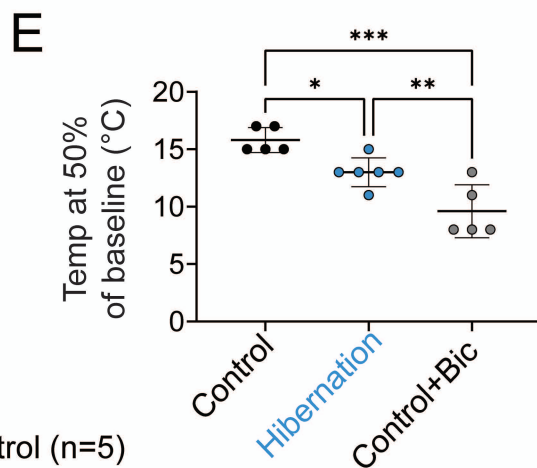
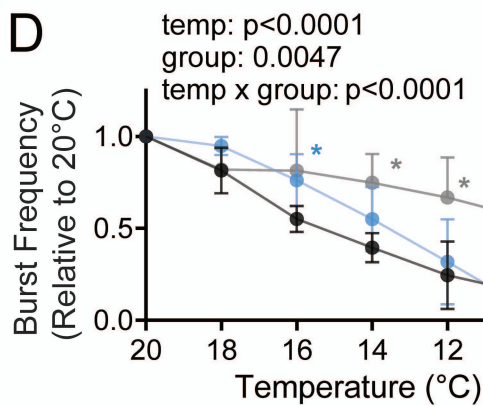
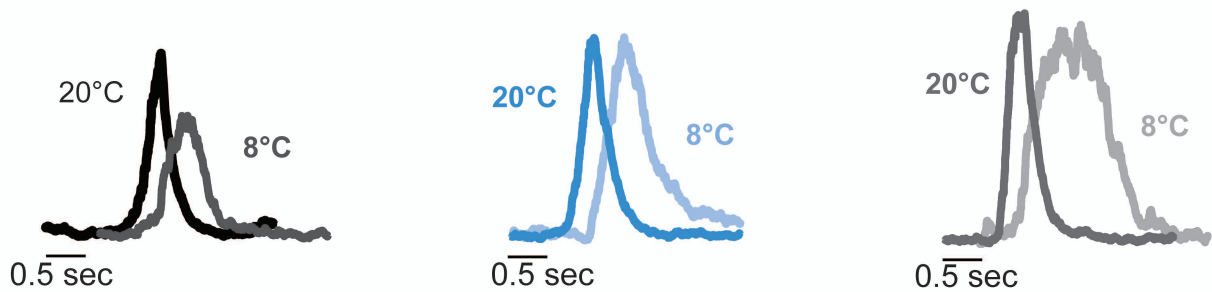
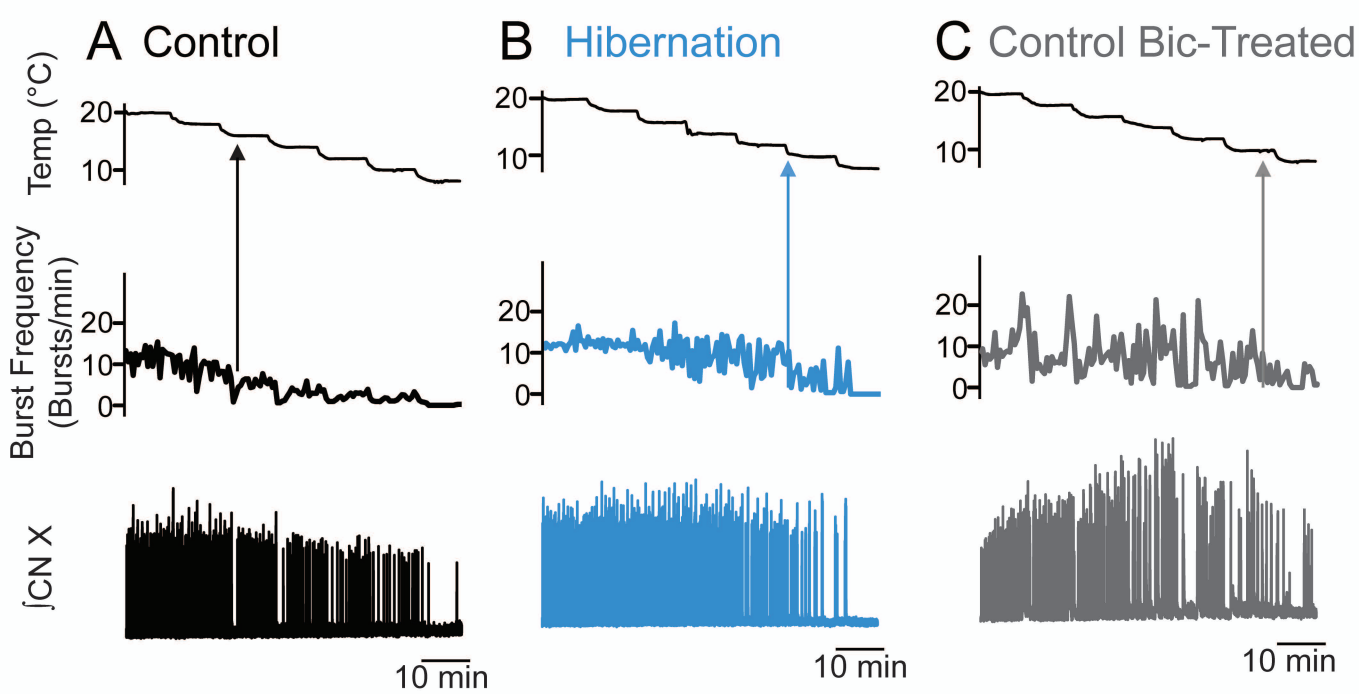
**A****B****C**

**A****B****C****D****E**

Control

Hibernation

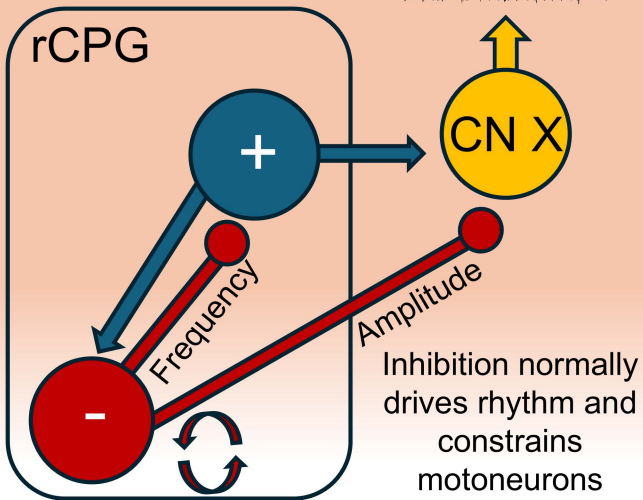




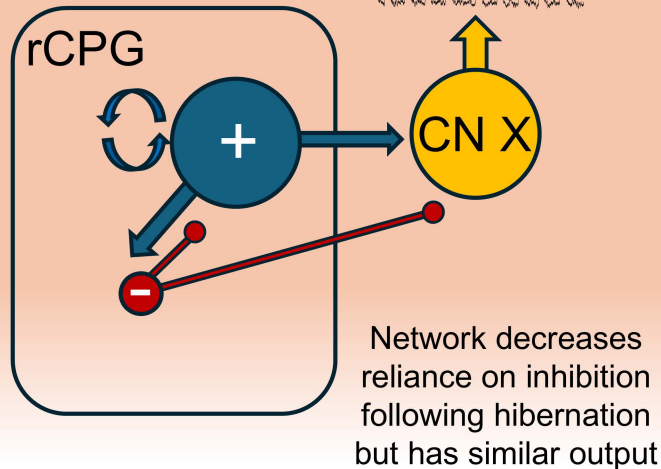


# Control

Warm

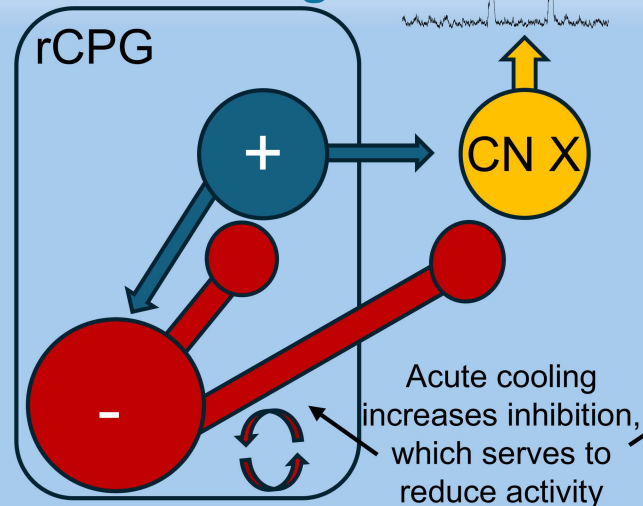


# Hibernation



# Control

Acute Cooling



# Hibernation

